MOUNTAIN-PLAINS CONSORTIUM

MPC 24-549 | R. Ghabchi and M. Mihandoust

EFFECT OF DEICING AGENTS AND ENVIRONMENTAL CONDITIONS ON THE PERFORMANCE OF ASPHALT PAVEMENTS IN COLD REGIONS

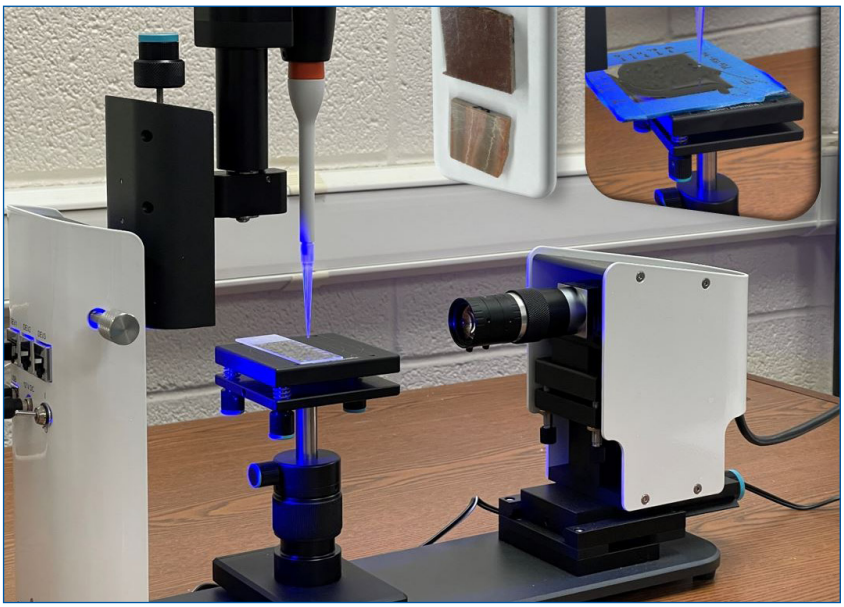

MOUNTAIN-PLAINS CONSORTIUM REGION 8

A University Transportation Center sponsored by the U.S. Department of Transportation serving the Mountain-Plains Region. Consortium members:

Colorado State University
North Dakota State University
South Dakota State University
University of Colorado Denver
University of Denver
University of Utah
Utah State University
University of Wyoming

Technical Report Documentation Page

1. Report No.	2. Government Accession No.	3. Recipient's Catalog No.
MPC-625		

4. Title and Subtitle	5. Report Date
Effect of Deicing Agents and Environmental Conditions on the Performance of Asphalt Pavements in Cold Regions	August 2024
	6. Performing Organization Code

7. Author(s)	8. Performing Organization Report No.
Rouzbeh Ghabchi Maryam Mihandoust	MPC 24-549

9. Performing Organization Name and Address	10. Work Unit No. (TRAIS)
South Dakota State University Box 2219, Crothers Engineering Hall, Rm. 310 Brookings, SD 57007	11. Contract or Grant No.

12. Sponsoring Agency Name and Address	13. Type of Report and Period Covered
Mountain-Plains Consortium North Dakota State University PO Box 6050, Fargo, ND 58108	Final Report
	14. Sponsoring Agency Code

15. Supplementary Notes

Supported by a grant from the US DOT, University Transportation Centers Program

16. Abstract

Pavements in cold regions of the United States undergo significant accumulation of snow and ice on their surfaces during the extended winter season, leading to reduced skid resistance and increased traffic crashes. Deicers, such as sodium chloride, calcium chloride, and magnesium chloride, have been used to remove ice as part of winter maintenance measures. However, their use combined with freeze-thaw (F-T) cycles and the interactions of these factors with the pavement components is linked to durability issues and premature failures. These interactions result in the debonding of asphalt binder and aggregate in the presence of chloride deicers and F-T cycles. The pull-off strength of PG 58-34 asphalt binder-aggregate systems conditioned with different aqueous concentrations of deicers subjected to F-T cycles was determined at the component level. Furthermore, the thermodynamic-based approach was used to assess the adhesion, debonding, and moisture-induced damage potential of aggregate-binder systems in the presence of deicer solutions. On the mix-level, the moisture-induced damage potential and the rutting resistance of the PG 58-34 asphalt mix specimens conditioned with salt solutions and F-T cycles were evaluated using the tensile strength ratio and Hamburg wheel tracker tests. A semicircular bend test was used to characterize the fracture properties of the asphalt mixes subjected to salt solutions and F-T. This multi-scale study intends to offer valuable insights into the adhesion and moisture-induced damage mechanisms of asphalt mix components when exposed to calcium chloride deicers and F-T cycles, contributing to developing effective winter maintenance plans for more durable pavements in cold areas.

17. Key Word	18. Distribution Statement
asphalt pavements, deicing chemicals, durability, environmental impacts, freeze thaw durability, frigid regions, pavement performance, winter maintenance	Public distribution

19. Security Classif. (of this report)	20. Security Classif. (of this page)	21. No. of Pages	22. Price
Unclassified	Unclassified	44	n/a

Form DOT F 1700.7 (8-72) Reproduction of completed page authorized

EFFECT OF DEICING AGENTS AND ENVIRONMENTAL CONDITIONS ON THE PERFORMANCE OF ASPHALT PAVEMENTS IN COLD REGIONS

Rouzbeh Ghabchi, Ph.D., P.E.
Associate Professor
Department of Civil and Environmental Engineering
South Dakota State University
Brookings, SD 57007

Maryam Mihandoust
Graduate Research Assistant
Department of Civil and Environmental Engineering
South Dakota State University
Brookings, SD 57007

August 2024

Acknowledgment

The study presented herein was conducted with support from the Mountain-Plains Consortium (MPC), a University Transportation Center funded by the United States Department of Transportation through project MPC-625. Contributions of the Ingevity Co., Bowes Construction Co., Jebro Co., Flint Hills Co., and GCC Ready Mix Co. are highly appreciated.

Disclaimer

ABSTRACT

Pavements in cold regions of the United States undergo significant accumulation of snow and ice on their surfaces during the extended winter season, leading to reduced skid resistance and increased traffic crashes. Deicers, such as sodium chloride, calcium chloride, and magnesium chloride, have been used to remove ice as part of winter maintenance measures. However, their use combined with freeze-thaw (F-T) cycles and the interactions of these factors with the pavement components is linked to durability issues and premature failures. These interactions result in the debonding of asphalt binder and aggregate in the presence of chloride deicers and F-T cycles. The pull-off strength of PG 58-34 asphalt binder-aggregate systems conditioned with different aqueous concentrations of deicers subjected to F-T cycles was determined at the component level. Furthermore, the thermodynamic-based approach was used to assess the adhesion, debonding, and moisture-induced damage potential of aggregate-binder systems in the presence of deicer solutions. On the mix-level, the moisture-induced damage potential and the rutting resistance of the PG 58-34 asphalt mix specimens conditioned with salt solutions and F-T cycles were evaluated using the tensile strength ratio and Hamburg wheel tracker tests. A semicircular bend test was used to characterize the fracture properties of the asphalt mixes subjected to salt solutions and F-T. This multi-scale study intends to offer valuable insights into the adhesion and moisture-induced damage mechanisms of asphalt mix components when exposed to calcium chloride deicers and F-T cycles, contributing to developing effective winter maintenance plans for more durable pavements in cold areas.

TABLE OF CONTENTS

LIST OF TABLES

LIST OF FIGURES

EXECUTIVE SUMMARY

More than 70% of the United States' roadway network is in regions subjected to severe winters, resulting in icy pavements that pose safety risks. Deicing, among different practices, is central to every winter maintenance effort. Deicing is defined as applying chemicals to facilitate the breaking up of the ice and snowpack and melting glare/black ice. Winter maintenance operations involving chloride-based deicers, such as NaCl, $CaCl_2$, and $MgCl_2$, are essential for ensuring road safety, mobility, and functionality. Deicing chemicals lower the freezing point and keep the precipitated water in the pavement in liquid form at freezing temperature. This, in turn, subjects the pavement to freeze-thaw cycles even during frigid temperatures. This mechanism accelerates moisture-induced damage, and pothole formation deteriorates asphalt pavements' durability and may negatively affect their structural integrity. Although there are growing concerns over the adverse effects of deicers on asphalt mixes, limited research has been conducted to address these concerns. Based on the need mentioned above, this study investigated the effects of commonly-used deicing agents on the durability and performance of asphalt mixes exposed to those chemicals and freeze-thaw cycles. More specifically, this study examined the effects of these deicers on adhesion evolution and moisture-induced damage mechanisms of asphalt binder-aggregate systems. The performance characteristics of the hot mix asphalt specimens, including rutting, moisture-induced damage, and cracking resistance, subjected to different deicer solutions and freeze-thaw cycles, were evaluated. At the component level, the effect of the deicer type (NaCl, $CaCl_2$, and $MgCl_2$) and freeze-thaw cycles on adhesion and damage mechanisms responsible for moisture-induced damage were assessed. At the micro-scale, a thermodynamic-based surface free energy method was pursued to characterize the adhesion and debonding energies and the moisture-induced damage potential of the binder-aggregate systems for different aggregates and asphalt binders in contact with various deicer solutions. According to the study's findings, elevated salt concentrations of deicer solutions led to a deterioration of adhesive and cohesive bonds between asphalt binder and aggregate systems in different scales. However, lower concentrations had an even more damaging effect due to their high ion mobility, allowing them to penetrate the asphalt mix and binder's internal structure. This infiltration induced chemical aging and altered the asphalt binder's microstructure via salt erosion. The effects of this phenomenon were observed on multiple testing scales, and the results from the various testing scales corroborated one another, supporting the findings. The outcomes of this study will help transportation agencies and highway authorities understand the adverse effects of deicers on pavement performance. This will help with the decision-making process of selecting the type of deicing agents to minimize any damage to asphalt pavement structures in cold climates.

1. INTRODUCTION

1.1 Problem Statement

Winter maintenance is vital in keeping the highway system and airport pavements safe and functional during winter. More specifically, the pavements in regions subjected to harsh and extended winter periods, such as those in North Central states, need more attention to keep the traffic flowing. Deicing, among different practices, is central to every winter maintenance effort. Deicing is defined as "the application of chemicals in order to facilitate breaking up the ice and snow pack and melting glare/black ice" (MnDOT, 2019). While sodium chloride (NaCl) is widely used as a deicing agent, other chemicals, namely calcium chloride ($CaCl_2$), magnesium chloride ($MgCl_2$), potassium chloride (KCl), and acetates, are also being used for ice removal, depending on their effectiveness in different temperature ranges (NHDES, 2016; USGS, 2016a,b; USGS, 2015; Sumsion and Guthrie, 2013; AGS, 2017). Deicing chemicals lower the freezing point and keep the precipitated water in the pavement in liquid form at freezing temperature. This, in turn, subjects the pavement to freeze-thaw cycles even during frigid temperatures. This mechanism accelerates moisture-induced damage and pothole formation (Hassan et al., 2002), deteriorates asphalt pavements' durability, and negatively affects their structural integrity. Although there are growing concerns over the adverse effects of deicers on asphalt mixes, limited research has been conducted to address these concerns (Hassan et al., 2002; Goh et al., 2011; Shi et al., 2009). Based on the need mentioned earlier, this study investigated the effects of commonly-used deicing agents on the durability and performance of asphalt mixes exposed to those chemicals and freeze-thaw cycles. The outcomes of this study will help transportation agencies and highway authorities better understand any possible adverse effects of using deicers on pavement performance. This will help with the decision-making process of selecting the type of deicing agent to minimize damage to asphalt pavement structures in cold climates.

1.2 Research Objectives

This study's primary goal is to investigate the mechanisms through which chloride salt solutions of different types and concentrations and F-T cycles impact the mechanical and adhesion properties of asphalt mixes, leading to moisture-induced damage using a multi-level characterization approach. The specific objectives of this study were as follows.

1. Investigate the rutting and stripping resistance and moisture-induced damage potential of a hot mix asphalt (HMA) containing a PG 58-34 asphalt binder conditioned with aqueous NaCl, $MgCl_2$, and $CaCl_2$ solutions with different concentrations, namely 0:1, 1:10, and 1:4 (volume of eutectic aqueous salt solution volume to volume of water) subjected to 7 F-T cycles by conducting tensile strength ratio (TSR) and Hamburg wheel tracker (HWT) test.
2. Evaluate the cracking resistance of an HMA mix conditioned with aqueous salt solutions of different eutectic concentrations (0:1, 1:10, and 1:4) and seven F-T cycles by conducting the semicircular bend (SCB) test.
3. Evaluate the evolution of adhesion and failure mechanisms in quartzite and PG 58-34 asphalt binder specimens conditioned with different aqueous eutectic concentrations salt solutions (0:1, 1:10, 1:15, 1:4, and 1:0) and seven F-T cycles using binder bond strength (BBS) test.
4. Investigate the moisture-induced damage potential of quartzite and PG 58-34 binder systems subjected to aqueous salt solutions of different eutectic concentrations (0:1, 1:15, 1:10, 1:4, and 1:0) using the surface free energy (SFE) approach.

1.3 Scope and Significance of Study

The effect of exposing asphalt mix and asphalt binder to different aqueous concentrations of chloride-based deicing salts (NaCl, $MgCl_2$, and $CaCl_2$), namely 1:0, 1:10, and 1:4 (by volume of eutectic solutions: water volume), and F-T cycles on their physical and mechanical properties, bonding characteristics, and failure mechanisms were evaluated. More specifically, the effect of the deicers and F-T cycles on mix characteristics, such as resistance to rutting, fatigue cracking, and moisture-induced damage potential, were evaluated for a Superpave mix containing a PG 58-34 asphalt binder and quartzite aggregates. The moisture-induced damage potential of dry and conditioned asphalt mixes was characterized by conducting the TSR test following the AASHTO T 283 standard procedure and the HWT test following the AASHTO T 324 standard method (AASHTO, 2022a,b). Outcomes of the HWT test were also used to determine resistance of the mixes (both non-conditioned and conditioned) to rutting. In addition, SCB tests conducted on the conditioned and non-conditioned asphalt mixes following the ASTM D 8044 standard method were used to determine the resistance of the mixes to fatigue cracking (ASTM, 2017). At the component level, the binder bond strength (BBS) test was conducted on asphalt binder-aggregate specimens prepared using a PG 58-34 asphalt binder and quartzite. The BBS tests were carried out according to the AASHTO T 361 standard method on the specimens in dry conditions and after conditioning them with aqueous solutions of salts prepared at 0:1, 1:15, 1:10, 1:4, and 1:0 concentrations (by volume of eutectic solutions: water volume) and F-T cycles standard method (AASHTO, 2022c). In addition, the failure mechanisms and their extents were investigated by analyzing the failure interface. To further explore the thermodynamical nature of the debonding mechanism in the presence of salt solutions, the SFE components of the PG 58-34 asphalt binder were determined by measuring its contact angles with three probe liquids with known SFE components. Similarly, SFE components of salt solutions of different concentrations were determined by measuring their contact angles with three solids of known SFE components. The interfacial energy parameters, such as work of adhesion, work of debonding, and energy ratios, were calculated for different salt concentrations to gain a multiscale understanding of the adhesion and stripping mechanisms and moisture-induced damage potential of aggregate-binder systems and mixes in the presence of moisture and deicer salts subjected to F-T cycles as a major step toward developing materials and methods to combat moisture and deicer-accelerated pavement distresses.

1.4 Report Organization

This report is organized in the following order:

Chapter 1: Introduction – This chapter includes the problem statement, research objectives, research scope, and organization of the report.

Chapter 2: Background –This chapter summarizes the literature review, focusing on the methods used to characterize the effects of deicing agents and moisture-induced damage on asphalt mixes.

Chapter 3: Materials and Methods – This chapter describes the selection and collection of the materials, sample preparation in the laboratory, and methodologies used for the laboratory characterization of the asphalt mixes subjected to different decers and the F-T cycles.

Chapter 4: Results and Discussions: Results of testing asphalt binders, asphalt binder-aggregate systems, and the asphalt mixes are summarized and presented in this section. More specifically, this chapter presents the outcomes of the BBS, SFE, SCB, HWT, and TSR tests.

Chapter 5: Conclusions and Recommendations– Important findings of this study and the recommendations based on these findings are presented in this chapter.

2. BACKGROUND

The asphalt mix is the primary material used in pavement construction, accounting for 93% of the 2.7 million miles of paved roads in the United States (NAPA, 2023). The extensive use of asphalt for pavement construction is due to its advantages, such as smoother surface for a better ride quality compared to other road construction materials, minimal noise, durability, high construction speed, lower cost compared to other pavement materials, options for and ease of maintenance (Feng et al., 2022; Pang et al., 2018). A significant concern for pavements in cold regions, such as northern and northcentral states, is maintaining their safety and serviceability after snowfall or ice formation during the cold season. According to the Federal Highway Administration (FHWA), icy pavements contribute to more than 150,000 crashes yearly (FHWA, 2023). This is predominantly due to reduced skid resistance, which leads to increased traffic incidents. Moreover, the economic losses caused by these problems are substantial (Shan et al., 2021; Han et al., 2019; Luo and Yang, 2015).

The development of snow melting and deicing methods, known as winter maintenance strategies, has received attention from highway and road agencies and has given them financial resources (Nixon and Williams, 2001). These technologies include mechanical, chemical, and manual snow removal methods. Among these strategies, the application of chemical deicers to prevent ice formation and removal is the most commonly used winter maintenance technique implemented by almost all state departments of transportation and highway authorities (Muthumani et al., 2017).

According to data from the United States Geological Survey (USGS), over 24 million metric tons of deicers, mainly sodium chloride and calcium chloride, are used annually (Kolesar et al., 2018). The typical road salt has been reported to reduce crashes on four-lane roads by 93% (FHWA, 2023). A chloride salt-water solution system can reduce the water's freezing point to temperatures much lower than pure water’s freezing point. However, the effectiveness of the chloride salts varies, depending on type. For example, when temperatures are expected to drop very low, applying calcium chloride as a deicer is more effective than sodium chloride as the former drops the freezing temperature more than the latter (Ketcham et al., 1996). Deicers directly lower the freezing point of water, allowing the ice to melt and weakening the bond between ice and pavement to facilitate its mechanical removal (Muthumani et al., 2017; Yang et al., 2018). The addition of deicer to snow causes the ice to thaw and, as thawing progresses, the liquid water content increases, resulting in the dilution of the deicer solution (Wåhlin et al., 2014; Atkin and De Paula, 2006). Therefore, changes in moisture and temperature regimes cause the pavement surface to undergo repeated freeze-thaw (F-T) cycles (Sarsembayeva and Collins, 2017). The combined effect of moisture, deicer, and F-T cycles can cause expansion and contraction, which shortens the service life of the pavement and causes failure modes, such as cracks and potholes (Choi, 2007; Teguedi et al., 2017).

These failures occur due to a primary form of distress in asphalt mixes known as moisture-induced damage, which can cause durability loss in the asphalt mix. Moisture-induced damage occurs due to the loss of adhesive bonds between the aggregate surface and asphalt binder (adhesive failure) and the loss of cohesive bonds within the asphalt binder (cohesive failure) in the presence of water (Caro et al., 2010a; Kakar et al., 2015). When moisture comes into contact with the asphalt binder, water can enter the spaces between the asphalt binder and aggregate, weakening the adhesive bond and, ultimately, separating the asphalt binder from the aggregate. This phenomenon is known as stripping (Kakar et al., 2015). Attempts have been made to characterize the moisture-induced damage mechanisms; however, due to their complexity, it is assumed that the debonding of aggregate-binder systems in the presence of water is not the result of a single mechanism but rather the interaction of multiple mechanisms (Mihandoust and Ghabchi, 2024, 2023; Ghabchi et al., 2016; Caro et al., 2010a; Kim et al., 2004; Kakar et al., 2015).

One of the most conventional mechanical laboratory tests developed for assessing the moisture-induced damage potential of asphalt mixes is the tensile strength ratio (TSR) test. This method consists of obtaining the ratio of the tensile strength of moisture-conditioned specimens over those of dry specimens. This ratio is used to predict the field moisture-induced damage potential for a mix following the AASTHO T283 standard procedure (Lottman, 1982; AASHTO, 2022a). Despite the extensive use of TSR for assessing moisture-induced damage in the past, it has certain shortcomings. One of its shortcomings is an inability to identify the material and failure mechanism responsible for moisture-induced damage. Therefore, predicting the potential for moisture-induced damage in a mix may be limited under field conditions. In addition, The TSR test lacks the calibration or standardization required for testing specimens of asphalt mix with decider solutions as the test is conducted for specimens conditioned with water following the AASHTO T283 standard procedure (Yang et al., 2021; Ali et al., 2022). Another test method developed to assess the moisture-induced damage potential and rutting resistance of the asphalt mixes is the Hamburg Wheel Tracker (HWT) test. Several transportation agencies have adopted the HWT test as an alternative to traditional TSR testing (Tavassitu and Baaj., 2020). This method measures rut depth caused by steel wheels passing on asphalt mix specimens submerged in water per AASHTO T324 standard procedure (AASHTO, 2022b). Due to the complicated effects of permanent deformation and stripping on rut-depth measurements, especially for asphalt mixes susceptible to moisture-induced damage, relying on rut-depth data may not accurately estimate mix rutting resistance. As a result, a considerable rut depth may indicate a mix susceptible to rutting, moisture-induced damage, or both (Yin et al., 2014; Yin et al., 2020). Due to the weakened aggregate-binder adhesive bond, moisture-induced damage may also exacerbate cracking failure observed in pavements, such as fatigue cracking. The semi-circular bending (SCB) test has been developed to address this form of failure by characterizing the fracture properties of the asphalt mix during cracking propagation following ASTM D 8044 standard procedure (ASTM, 2017). This test evaluates fatigue cracking from a crack initiation point of view using the tensile stress developing around the tip of a pre-existing notch and its fracture toughness (Safazadeh et al., 2022). Many studies have used mechanical mix tests to assess the effect of moisture, deicers, and F-T cycles on asphalt mix's moisture-induced damage potential, rutting, and cracking resistance.

Behbahani et al. (2020) evaluated the effect of different deicer solutions, including NaCl, on the moisture-induced damage potential and fatigue life of modified asphalt mixes with nano-hydrated lime. It was found that after calcium magnesium acetate (CMA), specimens moisture-conditioned with NaCl solutions had the highest TSR values compared to the other deicers. Wang et al. (2021) evaluated the effect of five different concentrations of sodium chloride deicer and freeze-thaw cycles on the moisture-induced damage potential of the mix, indicating that TSR values initially decrease with an increase in the NaCl concentration, then tend to be flat. Juli-Gándara et al. (2019) conducted TSR and HWT tests on asphalt mixes and reported when the aggregates were saturated in NaCl solutions, the mixes' TSR and permanent deformations were worse than other mixes not conditioned by salt solutions. Jiang-san et al. (2022) found increasing the number of freeze-thaw cycles may increase the accumulation rate of fatigue damage in warm mix asphalt (WMA). They concluded freeze-thaw cycles of more than 15, or the concentration of the NaCl solution of more than 4%, had an apparent effect on the growth of micro-cracks.

Similarly, Guo et al. (2022a) highlighted the effect of F-T cycles on modified asphalt mixes and indicated that F-T cycles worsen the fatigue performance of the mixes. In contrast, Ogbon et al. (2022) reported sodium chloride conditioning increased the mix stiffness, reducing rutting damage and fatigue damage in polymer-modified asphalt mixes. Zhang et al. (2022a,b) indicated a salt solution concentration greater than 6% and the number of freeze-thaw cycles of more than six, regardless of salt concentration, resulted in TSR values below the minimum requirement. Fakhri et al. (2019) evaluated the effects of chloride-based deicers, namely sodium chloride and magnesium chloride, on the moisture-induced damage potential of warm mix asphalt (WMA) using the TSR test. They reported the minimum reduction of tensile strength value was caused by sodium chloride and magnesium chloride, respectively.

The mechanics of aggregate-binder interface bonding significantly impact the response of the asphalt mix to moisture-induced damage (Kakar et al., 2015). Therefore, it is crucial to directly evaluate the adhesive- and cohesive-bond strengths at this interface. The binder bond strength (BBS) test is a commonly used pull-off test that has successfully assessed the adhesion and cohesion properties of the aggregate-binder interface (Ghabchi and Castro, 2022; Ghabchi and Castro, 2021a,b; Kakar et al., 2015; Moraes et al., 2011; Yan et al., 2016). This method measures the pull-off strength (POS) for the aggregate-binder specimens. While producing repeatable and reliable results, this test can determine the failure potential, mechanism, and extent in addition to the bond strength of asphalt binder and aggregate (Canestrari et al., 2010). Yee and Hamzah (2019) used the BBS test to evaluate the effect of anti-stripping fillers, F-T cycles, and aging on the moisture-induced damage potential of warm mix asphalt (WMA). They reported long-term aging and freeze-thaw cycles increased the extent of adhesive failure. Asif et al. (2018) evaluated the bond strength of asphalt binder with different aggregate mineralogies using the BBS test. They found that reducing POS values for moisture-conditioned specimens led to a change in failure mechanisms from cohesive to adhesive (Asif et al., 2018). Chen et al. (2023) indicated an increase in NaCl concentration and the number of F-T cycles had a more detrimental effect on moisture-induced damage resistance and POS of the aggregate-binder scale than that of the binder scale and asphalt mix scale.

Given that moisture-induced damage in asphalt mixes is a complex phenomenon involving different processes — namely thermodynamic, chemical, physical, and mechanical — evaluating the micro-scale interactions at the component level between the asphalt binder and aggregate is crucial to gain a fundamental understanding of the adhesion mechanisms (Caro et al., 2010b; Kakar et al., 2015; Ghabchi et al., 2014). For this purpose, the thermodynamic approach and modern surface energy theories predict moisture-induced damage (Howson., 2011; Bhasin et al., 2007b; Hamedi and Moghadas Nejad, 2015). Surface free energy (SFE), a fundamental thermodynamic property of a material, is defined as the work needed to create a unit area of a new surface of a material in vacuum conditions (Van Oss et al., 1988; Howson, 2011). Using the SFE components of asphalt binder and aggregate, the binding and debonding potential of the aggregate-binder systems in different conditions can be evaluated.

The binding potential, assessed by the work of adhesion, determines adhesion between the asphalt binder and aggregate under dry conditions. At the same time, the work of debonding is the energy required to separate the asphalt binder from the aggregate in the presence of moisture (Bhasin and Little, 2007; Bhasin et al., 2007a). Many studies in the past have used the thermodynamic approach as a screening method for material selection and moisture-induced damage evaluation. For example, Bhasin et al. indicated how the surface free energy (SFE) method could serve as a helpful tool for evaluating and selecting different aggregate-binder systems that exhibit increased resistance to moisture-induced damage (Bhasin et al., 2007b). Moghadas Nejad et al. assessed the moisture-induced damage potential in 12 different aggregate-binder systems. Additionally, they conducted the TSR tests on the mix specimens of the same aggregate-binder systems, and they were successful in establishing a correlation between the SFE and TSR results (Moghadas Nejad et al., 2013). Similarly, Habal and Singh (2017) investigated 16 aggregate-binder systems using the SFE approach, finding the aggregate with the best resistance to moisture-induced damage and establishing relationships between SFE components and asphalt binder modification.

Despite the numerous established methodologies of evaluating the moisture-induced damage potential of aggregate-binder systems, there is still a need for a thorough multi-level characterization and analysis of adhesion development and moisture-induced damage mechanisms in the presence of moisture and chloride-based deicers combined with F-T cycles. There is a knowledge gap about the effects of all chloride-based deicers since most of the past research has primarily focused on sodium chloride. Therefore, this study seeks to close this gap by capturing the damage characteristics and adhesion evolution in asphalt binder and asphalt mix subjected to different concentrations of chloride deicers, namely calcium, magnesium, and sodium chlorides, and F-T cycles at component and composition levels.

3. MATERIALS AND METHODS

3.1 Materials

3.1.1 Deicer Salts

The granular calcium chloride ($CaCl_2$), magnesium chloride ($MgCl_2$), and sodium chloride (NaCl) deicers shown in Figure 3.1 were collected from a local supplier and used to prepare aqueous deicer solutions with different concentrations for conditioning asphalt mix and binder samples. Initially, the salt solutions at their eutectic concentrations were prepared. The eutectic concentrations of the $CaCl_2$, $MgCl_2$, and NaCl consisted of 29.8%, 21.6%, and 23.3% of each salt by their weights and water, resulting in freezing temperatures as low as -51°C, -33°C, and -21°C, respectively (Ketcham et al., 1996). The aqueous eutectic concentration of each salt is shown by 1:0 (volumetric mixture of eutectic salt solution: volume of water), which indicates one volumetric part of the eutectic salt solution and zero volumetric parts of water. Diluted salt solutions with 1:15, 1:10, and 1:4 concentrations were prepared by adding water to the eutectic solution. The 0:1 concentration represents pure water.

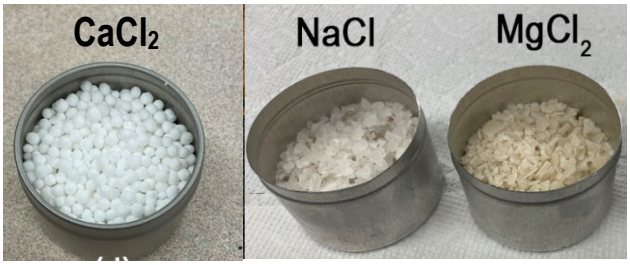

Figure 3.1 Photographic views of collected deicer salts

3.1.2 Asphalt Binder

The component level evaluations in this study were conducted using a PG 58-34 asphalt binder. The PG 58-34 asphalt binder, widely used in the northcentral states, was used to prepare the specimens required for conducting the binder bond strength test by following the AASHTO T 361 standard method and those needed for the SFE. The specific gravity of the used asphalt binder was 1.023. The 1-gallon asphalt binder canister was heated at 160°C to reach a liquid consistency and was poured into small cans, as presented in Figure 3.2, to be stored until specimen preparation.

Figure 3.2 A photographic view of the PG 58-34 asphalt binder sample in a small can

3.1.3 Aggregates

Aggregates' mineral composition significantly affects the adhesion between aggregate and asphalt binder (Cui et al., 2014). Therefore, it is essential to investigate the adhesive properties of the aggregate used in HMA production to resemble the mix type used in this study, which was quartzite, representing most of the aggregate mineralogy used in asphalt mixes in many states in the Midwest. Quartzite was collected in rock forms with a minimum of 300 mm dimension and cut with a tile saw to the required size, as shown in Figure 3.3.

Figure 3.3 A photographic view of the collected quartzite aggregate

3.1.4 Asphalt Mix

The asphalt mix used in this study was designed following Superpave requirements as per AASHTO M 323 (AASHTO, 2017a) standard specification and AASHTO R 35 (AASHTO, 2017b) standard practice for a traffic level of less than 0.3 million design equivalent single axle load (ESAL) in 20 years of service life (Figure 3.4). The asphalt mix consisted of 4.2% optimum virgin PG 58-34 asphalt binder content and 1.1% asphalt binder as a result of incorporating 20% reclaimed asphalt pavement (RAP), a total of 5.3% by the weight of the mix. The nominal maximum aggregate size (NMAS) of the HMA mixes was 12.5 mm, consisting of a blend of five different quartzite aggregate stockpiles and one RAP stockpile (Table 3.1). Other important volumetric parameters of the mix, namely void in mineral aggregates (VMA), voids filled with asphalt (VFA), and dust proportion (DP) values, were found as 15.1%, 73.5%, and 0.9%, respectively, all within the AASHTO M 323 (AASHTO, 2017a) requirements. This mix was produced in an asphalt plant, collected, and used to prepare the test specimens. The specimens of different geometries and dimensions needed for the mix performance tests were compacted in the laboratory in a Superpave gyratory compactor (SGC). The cylindrical specimens were sawed as needed to the shapes and dimensions specified by each test method. All performance tests were conducted on specimens having air voids of 7.0 ± 0.5%, representing the density of an asphalt layer right after construction.

Figure 3.4 A photographic view of the asphalt mix

Table 3.1 Gradations, mineralogies, and fractions of each aggregate stockpile in asphalt mix

Bin No. Mineralogy	Bin No. 1 Quartzite	Bin No. 2 Quartzite	Bin No. 3 Quartzite	Bin No. 4 Quartzite	Bin No. 5 Quartzite	RAP	Combined Gradation
% in Mix	12	8	32	12	16	20	
Size (mm)	Percentage Passing (%)						
19.0	100	100	100	100	100	100	100
15.9	95	95	100	100	100	99	99
12.5	66	88	100	100	100	97	94
9.5	35	48	100	100	100	94	87
4.75	6	6	82	100	100	78	71
2.36	2	2	65	71	83	60	55
1.18	2	2	48	49	61	46	41
0.6	2	2	31	33	42	35	28
0.3	1	1	15	18	23	23	15
0.075	1.0	1.0	6.1	1.9	2.2	9.9	4.7

3.2 Test Methods

3.2.1 Binder Bond Strength (BBS) Test

The BBS tests were conducted following the AASHTO T 361 standard method (AASHTO, 2022c) on asphalt binder-aggregate systems (Figure 3.5a). The BBS is a quick and reliable test method for evaluating the quality of binder-aggregate adhesion by measuring pull-off strength (POS) utilizing a pneumatic adhesion tensile testing instrument, PATTI. The BBS tests were conducted on dry and moisture-conditioned specimens. For moisture-conditioning of the BBS specimens, they were submerged in salt solutions of different concentrations, namely 1:0, 1:15, 1:10, 1:4, and 0:1, for 48 hours. The temperature of the solution was maintained at 25°C with a digital thermostat. Each specimen was sealed in a plastic bag containing 10 ml of the conditioning solution to prevent moisture from escaping the system. Using a programmable environmental chamber (Platinous P-300 Espec), plastic bags containing the specimens and solution were subjected to seven freeze-thaw (F-T) cycles. For each F-T cycle, the specimens underwent three hours of freezing at -18°C and three hours of thawing at 25°C. After the freeze-thaw cycles, the specimens were immersed in the conditioning solution at 25°C for two hours before testing. Dry specimens were tested at 25°C (Figure 5.2d), while the moisture-conditioned specimens were tested submerged in their respective conditioning solutions at 25°C, and pull-off strength (POS) values were measured. To this end, a pull-off force at a constant rate was applied to the pull stub using a PATTI. The test continued until failure, and the pull-off strength (POS) was recorded. Digital images of the aggregate-binder interface failure surfaces were examined to determine the failure

mechanisms by quantifying the adhesive and cohesive failure areas (Figure 3.5b). The results were reported as a percentage of the total area of the pull stub for each specific failure mechanism.

Additionally, the pull-off strength ratio (PSR) values were determined and reported by calculating the average POS value of the conditioned specimens to those of the dry specimens. The PSR values indicate the effect of salt solutions and F-T cycles on the adhesion between the aggregate and asphalt binder. Each BBS specimen set with different conditioning procedures and solution concentration combinations was tested with at least 11 aggregate-binder specimens.

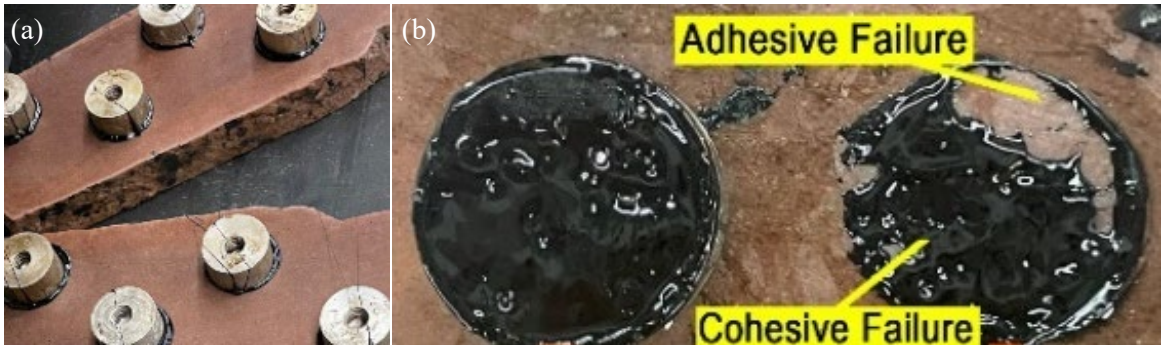

Figure 3.5 Photographic views of BBS test (a) pull stubs attached to the aggregate substrate; (b) adhesive and cohesive failures

3.2.2 Thermodynamic-Based Evaluation of Moisture-induced Damage

3.2.2.1 Surface Free Energy Concept

Good-Van Oss-Chaudhury's theory states a material's total SFE (Γ^{Total}) can be divided into a non-polar Lifshitz-van der Waals (Γ^{LW}) component and polar acid-base (Γ^{AB}) component, with acid-base component further subdivided into the Lewis acid component (Γ^{+}) and Lewis base component (Γ^{-}) as expressed by equation 3.1 (Good, 1992).

$$\Gamma^{Total} = \Gamma^{LW} + 2\sqrt{\Gamma^{+}\Gamma^{-}} \quad (3.1)$$

The binding potential of the asphalt binder (A) and aggregates (S) in dry conditions can be determined by the work of adhesion (W_{AS}), defined as the energy required to separate two phases of the interface to produce two as expressed in equation 3.2 (Bhasin et al., 2007b).

$$W_{AS} = 2\left(\sqrt{\Gamma_A^{LW}\Gamma_S^{LW}} + \sqrt{\Gamma_A^{-}\Gamma_S^{+}} + \sqrt{\Gamma_A^{+}\Gamma_s^{-}}\right) \quad (3.2)$$

The work of debonding (W_{ASW}^{Wet}), defined as the energy released through a thermodynamically favorable debonding of asphalt binder and aggregate in the presence of water (W), is determined from equation 3.3 (Bhasin and Little, 2007; 2009).

$$W_{ASW}^{Wet} = \Gamma_{AW} + \Gamma_{SW} - \Gamma_{AS} \quad (3.3)$$

The potential of an asphalt binder to coat the aggregate can be evaluated by wettability. The coefficient of spreading ($S_{A/S}$) is a quantitative measure of (wettability), which is presented in equation 3.4 (Zettlemoyer, 1968).

$$S_{A/S} = \Gamma_S - \Gamma_{AS} - \Gamma_A \quad (3.4)$$

As work of adhesion (W_{AS}) increases and the magnitude of work of debonding ($|W_{ASW}^{Wet}|$) decreases, the moisture-induced damage potential is reduced. Therefore, the energy ratio (ER_1) is used to express the work of adhesion and the work of debonding, as shown in equation 3.5 (Bhasin et al., 2007a).

$$ER_1 = \left|\frac{W_{AS}}{W_{ASW}^{Wet}}\right| \quad (3.5)$$

To account for the impact of wettability, Bhasin et al. (2007b) developed equation 3.6.

$$ER_2 = \left|\frac{S_{A/S}}{W_{ASW}^{Wet}}\right| \quad (3.6)$$

3.2.2.2 Asphalt Binder's SFE Components

The surface interfacial energies of a liquid (L) and a solid (S) can affect the contact angle (θ) of a liquid over a solid (Young, 1805). Therefore, the SFE components of the asphalt binder as the solid surface can be determined using the acid-base theory and Young-Dupre equation using equation 3.7 (Van Oss et al., 1988).

$$\Gamma_L(1+\cos\theta) = 2\left(\sqrt{\Gamma_L^{LW}\Gamma_S^{LW}} + \sqrt{\Gamma_L^{-}\Gamma_S^{+}} + \sqrt{\Gamma_L^{+}\Gamma_S^{-}}\right) \quad (3.7)$$

Equation 3.7, as a system of equations, can be solved for the measured contact angles of that solid with three probe liquids (polar, non-polar, bipolar natures) of known SFE components to determine the three unknown SFE components ($\Gamma_S^{LW}, \Gamma_S^{+}, \Gamma_S^{-}$) of any solid surface.

The sessile drop (SD) method, as a relatively simple technique providing accurate and reliable measurements, has been widely applied for direct measurement of contact angles of probe liquids with asphalt binder (Van Oss, 1994; Van Oss, 2002; Koc and Bulut, 2014). In this study, the SD method was used to measure contact angles of the probe liquids with asphalt binder to determine the SFE components of the asphalt binder.

The choice of probe liquids greatly influences the estimation of surface-free energy components of a material; therefore, probe liquids were selected based on condition number (CN) (Hefer et al., 2006; Little and Bhasin, 2007; Mishra et al., 2020). CN is a mathematical indicator of the sensitivity of the estimated SFE components to minor experimental errors in contact angle measurements (Hefer et al., 2006; Alvarez et al., 2012). Three probe liquids were selected for characterizing SFE components of asphalt binder with the lowest CN value, namely diiodomethane, ethylene glycol, and water. Table 5.2 presents the SFE components of the probe liquids (Good et al., 1990; Good and Van Oss, 1990; Van Oss et al., 1987).

Table 3.2 Surface free energy components of probe liquids at 20°C

Probe Liquids	Polarity	SFE Components of the Probe Liquids (mJ/m^2)				
		Γ^{LW} (non-polar)	Γ^{+} (acid)	Γ^{-} (base)	Γ^{AB} (acid-base)	Γ (total)
Diiodomethane (D)	Non-polar	50.8	0.0	0.0	0.0	50.8
Ethylene Glycol (E)	Polar	29.0	1.92	47.0	19.0	48.0
Water (W)	Bi-Polar	21.8	25.5	25.5	51.0	72.8

3.2.2.3 Salt Solutions' SFE Components

The SD method was used to measure contact angles of all three salt solutions, namely 1:15, 1:10, 1:4, and 1:0 (volume of eutectic aqueous salt solution to the volume of water) on probe solids with known SFE components. Using the measured contact angles and SFE components of three probe solids, three sets of equation 5.7 were solved to determine the SFE components of salt solutions (Van Oss et al., 1988). The three probe solids selected for this study were Polytetrafluoroethylene (PTFE) as a non-polar substrate, Poly(methyl methacrylate) (PMMA), a polar substrate, and the microscope glass slide as a substrate with bi-polar nature (Zdziennicka et al., 2017). Additionally, the contact angle measurements of the probe liquids (W-D-F) suggested by Zdziennicka et al. (2017) with probe solids were found to determine the SFE components of the probe solids using equation 3.7.

3.2.2.4 Preparation of Asphalt Binder Specimens for Sessile Drop Test

Square glass plates of 100 mm length and 2 mm thickness were cleaned with ethanol and distilled water, flamed using a Bunsen burner, and then used to prepare asphalt binder specimens. A small amount of PG 58-34 asphalt binder was heated to a liquid consistency in an oven at 160°C. Approximately 3g of the asphalt binder was placed on the glass plate and put inside the oven at 160°C for 15 minutes to allow the binder to spread and create a level and smooth surface (Figure 3.6a). Then, the asphalt binder specimen was stored for 24 hours at room temperature in a desiccator before being tested.

3.2.2.5 Contact Angle Measurement

Theta Lite OneAttension optical tensiometer (Biolin Scientific) was used for contact angle measurements (Figure 3.6b). The device was calibrated prior to each contact angle measurement. A 200-µL pipette was filled with probe liquid, and a droplet of 3-µL volume was carefully positioned on the solid surface at a drop rate of 2 µL/s. The contact angle measurements were recorded at a rate of 2 fps for 10 seconds until a steady angle was obtained, and the images were analyzed with the OneAttension built-in analysis software (Figure 3.6c). Then, the solid's surface free energy (SFE) components were calculated using the observed contact angles following the methodology discussed in section 3.2.2.2.

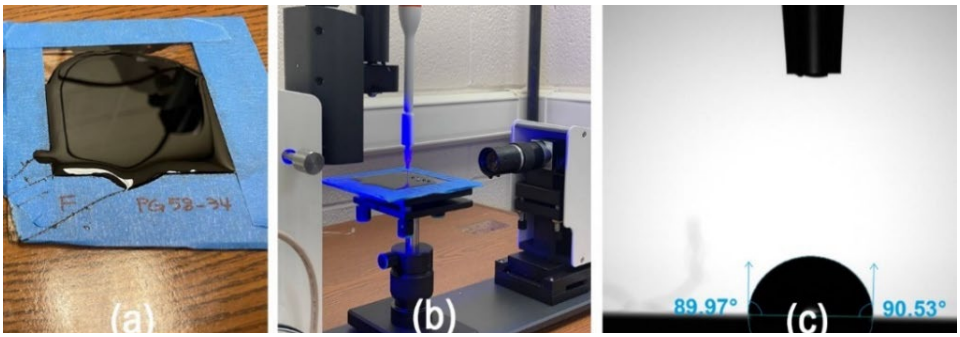

Figure 3.6 Photographic views of (a) prepared asphalt binder specimens, (b) conducting contact angle test on the asphalt binder specimen with an optical tensiometer, and (c) automatic digital contact angle measurement

3.2.3 Tensile Strength Ratio (TSR) Test

The TSR test was used to evaluate the moisture-induced damage potential of the mix specimens. TSR specimens of 95 mm height and 150 mm diameter were compacted following the AASHTO T 312 standard procedure (AASHTO, 2019). Four specimens were prepared for each test set and were moisture-conditioned following the AASHTO T 283 standard method (AASHTO, 2022a). The moisture-conditioning of the specimens included vacuum saturation in the corresponding salt solutions until reaching a saturation between 70 and 80% (AASHTO, 2022a). The specimens were placed in a sealed plastic bag with 10 ml of the same solution used for moisture-conditioning and placed in the environmental chamber for seven F-T cycles (Figure 3.7a). The specimens were submerged in their corresponding conditioning solution at 25°C for two hours before the test. The TSR tests were carried out by following the standard procedure in AASHTO T 283 (AASHTO, 2022a). Specimens were loaded at a constant rate of movement of 50 mm/min in the loading frame of an MTS tensile testing equipment at 25± 0.5 °C until failure, as seen in Figure 3.7b. The peak load at failure was recorded and used to calculate the tensile strength of each specimen using equation 3.8.

$$S_t = \frac{2000P}{\pi t D} \tag{3.8}$$

where, S_t = tensile strength (kPa); P = peak load at failure (N); t = specimen thickness (mm); and D = specimen diameter (mm).

The TSR value was determined by dividing the average tensile strength of moisture-conditioned specimens by those of the dry-conditioned specimens using equation 3.9.

$$TSR = \frac{S_{t\,(Wet)}}{S_{t\,(Dry)}} \tag{3.9}$$

where, $S_{t\,(Wet)}$ = tensile strength of moisture-conditioned specimens (kPa); and $S_{t\,(Dry)}$ = tensile strength of dry specimens (kPa).

Figure 3.7 Photographic views of (a) TSR specimens in the environmental chamber, (b) a TSR specimen during testing

3.2.4 Hamburg Wheel Tracker (HWT) Test

The HWT test was conducted to evaluate rutting and stripping potential of the mix specimens. For each set, four HWT specimens of 60 mm height and 150 mm diameter with 7.0% ± 0.5% air voids were prepared and tested for dry and moisture-conditioned specimens following the AASHTO T 324 test methods (AASHTO, 2022b). The HWT specimens were moisture-conditioned following the same procedure discussed in section 3.2.3. The specimens were cut to the required shape and tested using a Troxler two-wheel Hamburg wheel tracker (HWT) while submerged in water (Figure 3.8) at 50°C until 20,000 passes or a rut depth of 12.5 mm, whichever happened first. The recorded rut depth values were the average deformation from the right and left wheels measured at the midspan of each specimen set and the number of wheel passes measured and reported. The maximum permanent deformation and stripping inflection point (SIP), which serve as indicators of resistance to rutting and moisture-induced damage, were found through the test results analysis.

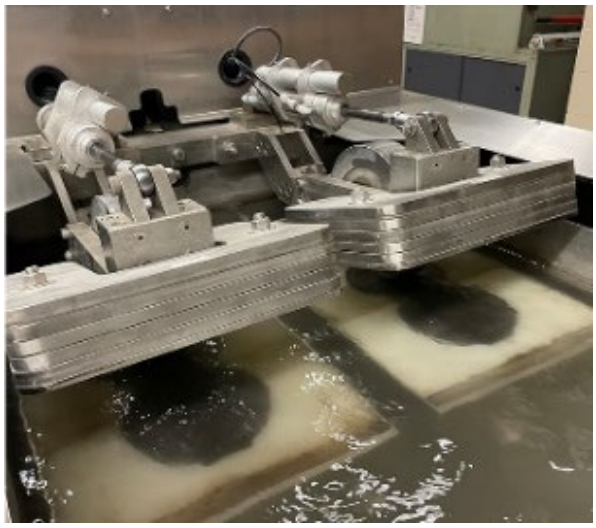

Figure 3.8 Photographic view of the submerged HWT specimens at 50ºC subjected to wheel loading

3.2.5 Semi Circular Bend (SCB) Test

The fracture potential of asphalt mixes was evaluated using the critical strain energy release rate (J_c) determined by the semi-circular bend (SCB) test. The semi-circular specimens of 7.0 ± 0.5% air voids were prepared and tested following the ASTM D 8044 standard procedure (ASTM, 2017). For this purpose, cylindrical specimens of 135 mm in height and 150 mm in diameter were compacted. The compacted specimens were marked and saw-cut at their mid-height. Each half was cut to a diameter of 150 mm and a height of 57±1 mm with two cut faces to minimize the variations caused by the irregularities of the compacted surface. Each cylindrical specimen was cut into four semi-circular specimens. The specimens' long-term temperature-conditioning (aging) for 120 hours at 85ºC was carried out according to AASHTO R30 (AASHTO, 2016) standard practice. The specimens were moisture-conditioned following the steps described in section 3.2.3 (Figure 3.9a). After the completion of F-T cycles, three nominal notch depths, namely 25mm, 32mm, and 38 mm, vertical to the rectangular base of the specimens, were cut, and the specimens were air-dried on a steel grid surface for 48 hours to avoid inflicting the heating-healing of the asphalt mix by drying it in the oven. SCB tests were conducted on dry and moisture-conditioned specimens using an asphalt mix performance tester (AMPT) inside an environmental chamber at 16°C intermediate temperature following ASTM D 8044, as shown in Figure 3.9b (ASTM, 2017). The specimens were kept inside the environmental chamber of the AMPT at the intermediate temperature for at least two hours before the test. After each test, load-deformation data for the SCB specimens were plotted for each notch depth. They were used to calculate the critical strain energy release rate, J_c, using equation 3.10. The area under the load-deformation curve was determined by the discrete integration method.

$$J_c = \frac{-1}{b}\left(\frac{dU}{da}\right) \tag{3.10}$$

where, J_c = critical strain energy release rate (kJ/m^2); b = specimen thickness (m); a = notch depth (m); U = strain energy to failure (kJ); and dU/da = change of strain energy with notch depth (kJ/m).

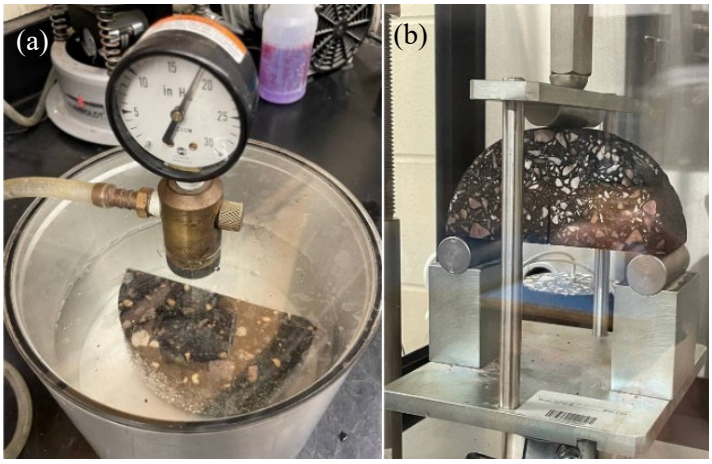

Figure 3.9 Photographic view of (a) semi-circular specimens during vacuum saturation and (b) a semi-circular bend specimen during the test

4. RESULTS AND DISCUSSION

4.1 Asphalt Binder-aggregate Tensile Bond Strength

The effects of different deicer salts with various concentrations and freeze-thaw (F-T) cycles on the adhesion between the asphalt binder and quartzite by conducting binder bond strength (BBS) test are summarized in this section. The results include the pull-off strength (POS) and the pull-off strength ratio (PSR) values obtained for BBS specimens of quartzite with PG 58-34 asphalt binder subjected to aqueous salt solutions with different concentrations and F-T cycles. Furthermore, based on the overall area of the pull stub and the areas with different failure modes, the extent of the cohesive and adhesive failure modes was assessed and provided as a percentage.

Table 4.1 presents the POS and PSR values for quartzite aggregate-PG 58-34 binder specimens in dry condition and specimens conditioned by different aqueous $CaCl_2$ concentrations, including 0:1 (pure water), 1:15, 1:10, 1:4, and 1:0 (ratio of eutectic $CaCl_2$ solution volume to volume of water) and subjected to 7 F-T cycles. Additionally, the observed failure mechanisms, namely cohesive and adhesive, as a percentage of the failure interface areas are shown in Table 4.1. The POS values of quartzite-binder specimens subjected to water and calcium chloride solutions with eutectic concentrations of 0:1 (pure water), 1:15, 1:10, 1:4, and 1:0 and 7 F-T cycles exhibited 11, 12, 2, 10, and 15% reduction compared to those of dry specimens, respectively. The most significant reduction in POS value (15%) pertains to specimens moisture-conditioned with the highest concentration of $CaCl_2$ (1:0). It was also observed that the primary failure mechanism of the quartzite-binder systems was cohesive while remaining between 93 to 100% for all tests, indicating the cohesive bond was more significantly affected than the adhesive bond. In the presence of higher $CaCl_2$ concentrations, the $CaCl_2$ concentration in the interior voids of the specimen reaches saturation conditions more readily than at lower concentrations. This saturation results in the crystallization of $CaCl_2$ and the subsequent growth of crystals within the asphalt binder. The crystallization and expansion of crystals apply tensile stresses on the surrounding asphalt binder, which can cause the voids within the asphalt binder to expand, thereby reducing the asphalt binder's cohesive strength. Furthermore, the crystal expansion pressure may cause micro-cracking in the asphalt binder, which might provide pathways for moisture infiltration, further compromising the cohesive tensile strength (Cui et al., 2017).

Previous studies have shown the component fractions of asphalt binder, namely resins, asphaltenes, aromatics, and saturates, change when moisture-conditioned with chloride ions (Qian et al., 2021). The resins and asphaltenes increase while the aromatics and saturate decrease; therefore, the asphalt binder becomes stiffer as it goes through a chemical aging process and negatively impacts the cohesive bonds within asphalt binder (Pang et al., 2018; Qian et al., 2021). In the mineralogy of quartzite, the high quartz content (>90%) may play an essential role in establishing a strong adhesive bond with asphalt binder. Previous research indicates that asphaltenes, the polar components of asphalt binder, exhibit strong adhesion with quartz (Du and Zhu, 2019). In addition, determining the aggregate's nature (acidic or basic) can provide more insight into its adhesion quality and compatibility with asphalt binder, as discussed in section 5.6.2. In the same section, the potential of $CaCl_2$ solutions to penetrate aggregate-binder interfaces using the SFE method was also investigated.

Table 4.1 Summary of POS and PSR values and failure mechanisms observed in the BBS specimens prepared using PG 58-34 asphalt binder and quartzite aggregate conditioned with different concentrations of $CaCl_2$ salt and F-T cycles

F-T Cycles	Conditioning Solution Volumetric Eutectic $CaCl_2$ Solution:Water	Asphalt Binder Type: PG 58-34 Aggregate Type: Quartzite			PSR Value (POS_{Wet}/POS_{Dry})
		POS (kPa)	COV (%)	Failure Type (% Cohesive)	
0	None (dry)	468.6	3.4%	100%	-
7	0:1 (pure water)	418.4	7.5%	100%	0.89
7	1:15	414.6	7.2%	100%	0.88
7	1:10	457.9	2.6%	93%	0.98
7	1:4	423.7	8.0%	100%	0.90
7	1:0	396.6	2.5%	97%	0.85

Table 4.2 presents the POS and PSR values for quartzite aggregate-PG 58-34 binder specimens in dry condition and specimens conditioned by different aqueous $MgCl_2$ concentrations, including 0:1 (pure water), 1:15, 1:10, 1:4, and 1:0 (ratio of eutectic $MgCl_2$ solution volume to volume of water) and subjected to seven F-T cycles. Additionally, the observed failure mechanisms, namely cohesive and adhesive, as a percentage of the failure interface areas are shown in Table 4.2. It was observed that the POS values of the specimens conditioned with $MgCl_2$ aqueous solutions of 0:1(pure water), 1:15, 1:10, 1:4, and 1:0 concentrations, and seven F-T cycles were reduced by 2, 18, 1, 32, and 22% respectively. As a result, a general decrease in POS values was observed for the specimens conditioned with moisture. Notably, specimens conditioned with a 1:4 concentration of $MgCl_2$ exhibited the highest loss in POS value, reaching 32%, followed by specimens conditioned with a 1:0 concentration, which exhibited a 22% loss in POS value.

Furthermore, Table 4.2 demonstrates a substantial change in failure mechanism from cohesive to adhesive for concentrations greater than 1:15. In the concentrations of 1:4 and 1:0, where POS was most negatively impacted, 100% adhesive failures were recorded, indicating the loss in POS was predominantly attributable to a weakening of the adhesive bonds. This finding indicates the high concentration of $MgCl_2$ had a negative effect on the adhesive bonds. This is due to moisture infiltration into the asphalt binder via adsorption, replacement, and diffusion mechanisms, weakening the aggregate-binder interface adhesive bond (Zhou et al., 2021).

Table 4.2 Summary of POS and PSR values and failure mechanisms observed in the BBS specimens prepared using PG 58-34 asphalt binder and quartzite aggregate conditioned with different concentrations of $MgCl_2$ salt and F-T cycles

F-T Cycles	Conditioning Solution Volumetric Eutectic $MgCl_2$ Solution:Water	Asphalt Binder Type: PG 58-34 Aggregate Type: Quartzite			PSR Value (POS_{Wet}/POS_{Dry})
		POS (kPa)	COV (%)	Failure Type (% Cohesive)	
0	None (dry)	468.6	3.4%	100%	-
7	0:1 (pure water)	459.7	2.9%	100%	0.98
7	1:15	383.6	5.5%	100%	0.82
7	1:10	461.7	3.5%	49%	0.99
7	1:4	318.5	7.6%	0%	0.68
7	1:0	367.6	2.9%	0%	0.78

Table 4.3 presents the POS and PSR values for quartzite aggregate-PG 58-34 binder specimens in dry condition and specimens conditioned by different aqueous NaCl concentrations, including 0:1 (pure water), 1:15, 1:10, 1:4, and 1:0 (ratio of eutectic NaCl solution volume to volume of water) and subjected to seven F-T cycles. Additionally, the observed failure mechanisms, namely cohesive and adhesive, as a percentage of the failure interface areas are shown in Table 4.3. It was observed that the POS values of specimens conditioned with NaCl aqueous solutions of concentrations 0:1 (pure water), 1:15, 1:10, 1:4, and 1:0 subjected to seven F-T cycles were 2, 17, 4, 6, and 17% lower than those of the dry specimen, respectively. The specimens conditioned with the lowest concentration (1:15) and the highest concentration (1:0) of NaCl solutions experienced the highest reduction in POS values, with a 17% decrease for both. Analyzing the failure mechanisms presented in Table 4.3 for samples conditioned with NaCl solution reveals the failure mode observed at all concentrations was cohesive. Therefore, it is reasonable to conclude that NaCl negatively affected cohesive bonds. At low concentrations, F-T cycles result in expansion and crystallization owing to ice formation, exerting freezing expansion forces on the asphalt binder's internal structure when water freezes (Guo et al., 2019; Wu et al., 2023). Alternatively, at high concentrations (1:0 in this instance), the migration of NaCl into the asphalt binder due to osmotic pressure difference results in the reaction of NaCl with the binder in salt erosion (Zhang et al., 2022a; Wu et al., 2023). This salt erosion can change the asphalt binder's composition, decreasing the proportion of light components, such as saturated and aromatic fractions, while increasing the proportion of heavy components, such as resin and asphaltene fractions (Zhou et al., 2022; Zhang et al., 2022a). As a result, the asphalt binder undergoes aging, becomes more brittle, and ultimately becomes more prone to cohesive failure.

Table 4.3 Summary of POS and PSR values and failure mechanisms observed in the BBS specimens prepared using PG 58-34 asphalt binder and quartzite aggregate conditioned with different concentrations of NaCl salt and F-T cycles

F-T Cycles	Conditioning Solution Volumetric Eutectic NaCl Solution:Water	Asphalt Binder Type: PG 58-34 Aggregate Type: Quartzite			PSR Value (POS_{Wet}/POS_{Dry})
		POS (kPa)	COV (%)	Failure Type (% Cohesive)	
0	None (dry)	468.6	3.4%	100%	-
7	0:1 (pure water)	459.7	2.9%	100%	0.98
7	1:15	388.7	5.4%	100%	0.83
7	1:10	449.1	4.5%	100%	0.96
7	1:4	441.2	4.8%	100%	0.94
7	1:0	388.7	5.4%	100%	0.83

Notably, the PSR values of specimens conditioned with NaCl and $CaCl_2$ were higher than those observed for $MgCl_2$. This finding suggests that $MgCl_2$ had a more detrimental effect on the POS than other twp salts, as it was also found to have a more significant effect on the adhesion bond. This negative effect can be attributed to the Mg^{2+} ion's lower atomic radius than the Na^+ and Ca^+ ions, which potentially allows it to penetrate the interface more effectively than the Na^+ ion, leading to a higher degree of moisture-induced damage, adhesion failure, and debonding of aggregate-binder systems.

4.2 Surface Free Energy Parameters

4.2.1 SFE Components of Asphalt Binder

A summary of the contact angles measured on PG 58-34 asphalt binder using different probe liquids (W-E-D) and SFE components of PG 58-34 is shown in Table 4.4. At least 10 angles were measured for each probe liquid to assure accuracy. The mean value indicates the average of the reliable readings, and the coefficient of variance (COV) values are also given, showing the degree of fluctuation among the recorded contact angles. The readings were selected to maintain a coefficient of variation below 1% to guarantee they are reliable and repeatable, indicating their consistency and precision. The water exhibited the highest contact angle measurement of all probe liquids (104.96°). This observation was due to the bipolar nature of water, which resulted in a contact angle greater than 90 degrees with the non-polar and hydrophilic asphalt binder, indicating minimal wettability. In contrast, diiodomethane exhibited the smallest contact angle (47.51°) due to its non-polar properties, allowing it to spread on asphalt binder readily. Hence, the non-polar SFE component had the highest value for asphalt binder, highlighting its non-polar nature in agreement with those reported in the literature (Bhasin and Little, 2007; Bhasin et al., 2007a,b; Soenen et al., 2020; Zhang et al., 2018).

Table 4.4 Measured contact angles and SFE components of the PG 58-34 asphalt binder

Probe Liquids	Measured Contact Angles		SFE Components (mJ/m^2)	
	Mean (degrees)	COV(%)	Γ^{LW} (non-polar)	35.63
Diiodomethane	47.51	0.8	Γ^{+} (acid)	0.54
Ethylene Glycol	80.58	0.6	Γ^{-} (base)	0.31
Water	104.96	0.5	Γ (total)	36.45

4.2.2 SFE Components of Probe Solids

The SFE components of the probe solids were determined by measuring their contact angles with the probe liquids, consistent with the methodology discussed in section 3.2.2.2. Table 4.5 presents the SFE components of the glass, PMMA, and PTFE probe solids.

Table 4.5 Measured SFE components of the probe solids (glass, PMMA, PTFE)

Probe Solids	SFE Components (mJ/m^2)				
	Γ^{LW} (non-polar)	Γ^{+} (acid)	Γ^{-} (base)	Γ^{AB} (acid-base)	Γ (total)
Glass	32.0	1.8	22. 4	12.7	45.7
PMMA	41.1	0.0	9.6	1.0	42.1
PTFE	19.8	0.1	0.9	0.4	20.2

4.2.3 SFE Components of $CaCl_2$ Solutions

The measured contact angles of $CaCl_2$ solutions with different concentrations, namely 0:1 (pure water), 1:15, 1:10, 1:4, and 1:0 (volume of eutectic solution: volume of water) with probe solids (glass, PMMA, and PTFE), were used to determine the SFE components of the salt solutions. For each probe solid and salt concentration, a minimum of 10 measurements were taken, and the standard deviation values were also given to provide insight into the measurement variability. The surface free energy components of $CaCl_2$ solutions calculated based on the contact angle measurements are shown in Table 4.6. As the concentration of $CaCl_2$ rises, the acid, base, and acid-base SFE components tend to decrease. This finding implies that compared to solutions with lower concentrations, when the $CaCl_2$ concentration rises, the

total surface energy component of the $CaCl_2$ solutions reduces. In the presence of higher-concentration CaCl2 solutions, less energy is needed to create a new surface area; therefore, the solution may spread quickly onto the aggregates and the binder.

Table 4.6 Surface free energy components of $CaCl_2$ solutions

Aqueous $CaCl_2$ Concentration (Eutectic Solution: Water)	SFE Components (mJ/m^2)				
	Γ^{LW} (non-polar)	Γ^{+} (acid)	Γ^{-} (base)	Γ^{AB} (acid-base)	Γ (total)
0:1 (Water)	21.8	25.5	25.5	51.0	76.5
1:15	0.0	74.7	10.4	55.9	55.9
1:10	0.0	64.7	9.1	48.5	48.5
1:4	0.1	52.7	8.4	42.0	42.1
1:0	0.3	36.8	0.0	1.8	2.1

4.2.4 SFE Components of $MgCl_2$ Solutions

The measured contact angles of $MgCl_2$ solutions with different concentrations, namely 0:1 (pure water), 1:15, 1:10, 1:4, and 1:0 (volume of eutectic solution: volume of water) with probe solids (glass, PMMA, and PTFE), were used to determine the SFE components of the salt solutions. For each probe solid and salt concentration, a minimum of 10 measurements were taken, and the standard deviation values were also given to provide insight into the measurement variability. The surface free energy components of $MgCl_2$ solutions calculated based on the contact angle measurements are shown in Table 4.7. Using $MgCl_2$ solutions of 1:15, 1:10, 1:4, and 1:0 concentrations resulted in the total SFE component of the water (76.5 mJ/m^2) initially decreasing to 38.5 and subsequently increasing to 53.7, 66.1, and 101.3 mJ/m^2 respectively. Therefore, the total SFE of $MgCl_2$ solutions increased as the concentration increased.

Table 4.7 Surface free energy components of $MgCl_2$ solutions

Aqueous $MgCl_2$ Concentration (Eutectic Solution: Water)	SFE Components (mJ/m^2)				
	Γ^{LW} (non-polar)	Γ^{+} (acid)	Γ^{-} (base)	Γ^{AB} (acid-base)	Γ (total)
0:1 (Water)	21.8	25.5	25.5	51.0	76.5
1:15	0.0	79.3	4.7	38.5	38.5
1:10	0.0	57.5	12.5	53.7	53.7
1:4	0.0	51.4	21.2	66.1	66.1
1:0	0.3	23.3	109.8	101.1	101.3

4.2.5 SFE Components of NaCl Solutions

The measured contact angles of NaCl solutions with different concentrations, namely 0:1 (pure water), 1:15, 1:10, 1:4, and 1:0 (volume of eutectic solution: volume of water) with probe solids (glass, PMMA, and PTFE), were used to determine the SFE components of the salt solutions. For each probe solid and salt concentration, a minimum of 10 measurements were taken to minimize measurement variability. The surface free energy components of NaCl solutions calculated based on the contact angle measurements are shown in Table 4.8. From Table 4.8, it was observed that an increase in the concentration of NaCl in the solution led to a reduction in the total SFE component. As observed in Table 4.8, NaCl solutions of 1:15, 1:10, 1:4, and 1:0 concentrations resulted in the total SFE component of the water (76.5 mJ/m^2) decreasing to 52.8, 47.0, 37.0, and 15.8 mJ/m^2 respectively.

Table 4.8 Surface free energy components of NaCl solutions

Aqueous NaCl Concentration (Eutectic Solution: Water)	SFE Components (mJ/m^2)				
	Γ^{LW} (non-polar)	Γ^{+} (acid)	Γ^{-} (base)	Γ^{AB} (acid-base)	Γ (total)
0:1 (Water)	21.8	25.5	25.5	51.0	76.5
1:15	0	71.3	9.8	52.8	52.8
1:10	0	63.7	8.6	46.9	47.0
1:4	0.1	54.7	6.2	36.9	37.0
1:0	0.3	32.8	1.8	15.5	15.8

4.2.6 SFE Components of Aggregates

Measuring the contact angle between probe liquids and aggregates to determine the SFE components of aggregates through the sessile drop method has proven challenging due to variability caused by surface roughness of the aggregate (Drelich, 1997). Therefore, SFE components of quartzite were adopted from the literature, as seen in Table 4.9 (Arabani and Hamedi, 2011). The highest SFE component for quartzite aggregate was observed to be the basic component, indicating it is a relatively basic aggregate. Hydrophobic aggregates are considered to be chemically basic and tend to have a higher moisture-induced damage resistance than acidic aggregates (Tarrer and Wagh, 1991).

Table 4.9 Surface free energy components of quartzite (Arabani and Hamedi, 2011)

Aggregate Type	Literature Source	SFE Components (mJ/m^2)				
		Γ^{LW} (non-polar)	Γ^{+} (acid)	Γ^{-} (base)	Γ^{AB} (acid-base)	Γ (total)
Quartzite	Arabani and Hamedi (2011)	54.91	19.67	583.53	214.27	269.18

4.2.7 Energies of Adhesion and Debonding

The SFE components of the quartzite aggregate (Table 4.9) and those of the PG 58-34 asphalt binder (Table 4.4) were plugged into equations 3.2 and 3.4 to determine the work of adhesion and spreading coefficient of the two phases. As a result, the work of adhesion value for the PG 58-34 asphalt binder and quartzite in dry conditions was calculated as 128.8 mJ/m^2 and the spreading coefficient of PG 58-34 asphalt binder over quartzite was found as 55.92 mJ/m^2. In addition, the SFE components of asphalt binder (Table 4.4), SFE components of quartzite (Table 4.9), and SFE components of salt solutions with various concentrations (Tables 4.6, 4.7, and 4.8) and equation 3.3 were used to determine the work of debonding in the presence of the liquid phase for the aggregate-binder-salt solutions system. Table 4.10 presents a summary of the work of debonding values for quartzite and PG 58-34 asphalt binder when subjected to aqueous salt solutions of different concentrations, namely 0:1, 1:15, 1:10, 1:4, and 1:0 (volumetric parts of eutectic salt solution: volumetric parts of water).

For all deicers, an increase in solution concentration resulted in a rapid reduction and subsequent increase in the work of debonding (W_{ASW}^{Wet}) values. More specifically, the $CaCl_2$ solutions substantially reduced the work of debonding for aggregate-binder systems. In particular, the work of debonding values (W_{ASW}^{Wet}) for systems with $CaCl_2$ concentrations of 1:15, 1:10, 1:4, and 1:0 were 45.8, 26.4, 21.6, and 19.6% less than that of water. This observation suggests the magnitude of the work of debonding ($|W_{ASW}^{Wet}|$) increased, indicating that higher energy was released during the debonding of asphalt binder and aggregate in the presence of $CaCl_2$ solutions than water. Therefore, this thermodynamically favorable phenomenon makes the aggregate-binder system more susceptible to moisture-induced damage. The highest reduction in the work of debonding value was observed at the lowest (1:15) concentration (45.8%).

The W_{ASW}^{Wet} for aggregate-binder systems and $MgCl_2$ concentrations of 1:15, 1:10, 1:4, and 1:0 were 70.2 and 15.3% less and and 4.9 and 81.0% more than that of water, respectively. Therefore, the magnitude of the work of debonding ($|W_{ASW}^{Wet}|$) initially increased and then decreased, indicating that during the debonding of aggregate and binder in contact with $MgCl_2$ solution of different concentrations, the lowest concentration (1:15) exhibited the highest energy release (259.3 mJ/m^2) and the highest concentration (1:0) had the lowest energy release (28.9 mJ/m^2). Therefore, the aggregate-binder system was more susceptible to moisture-induced damage in lower concentrations of $MgCl_2$. However, it must be noted that the SFE approach does not characterize the mechanisms occurring due to F-T cycles. More specifically, it does not account for crystallization, expansion forces acting on the internal structure of asphalt binders due to F-T cycles, salt erosion, or the effects of asphalt binder's chemical aging in high concentrations of deicer solutions.

Additionally, it was observed that the W_{ASW}^{Wet} for aggregate-binder systems, NaCl concentrations of 1:15, 1:10, 1:4, and 1:0 were 44.6, 35.9, 29.5, and 0.7% less than water. Similarly, the lowest concentration (1:15) of NaCl resulted in the highest energy release during the debonding of aggregate and binder. Salt solutions have more mobility at low concentrations than those at higher concentrations. Therefore, migration and displacement of light fractions and the water-soluble layer of the asphalt binder are more facilitated (Prieve et al., 2019; Van Oss, 2008).

Table 4.10 Work of debonding for PG 58-34 asphalt binder, quartzite aggregate, and salt solutions

Aqueous Salt Concentration (Eutectic Solution: Water)	Work of Debonding (W_{ASW}^{Wet}) (mJ/m^2)		
	$CaCl_2$	$MgCl_2$	NaCl
0:1 (pure water without salt)	-152.3		
1:15	-222.1	-259.3	-220.3
1:10	-207.8	-175.7	-207.0
1:4	-185.3	-144.8	-197.2
1:0	-182.3	-28.9	-151.3

4.2.8 Effect of Aqueous Salt Solutions on Moisture-induced Damage Potential

The moisture-induced damage potential and compatibility of the asphalt binder, aggregate, and salt solutions were evaluated using energy ratio parameters ER_1 and ER_2. To this end, the work of adhesion, work of debonding, spreading coefficient values, and equations 3.5 and 3.6 were used to determine the energy parameters ER_1 and ER_2, as summarized in Table 4.11. Overall, the ER_1 and ER_2 parameters exhibited similar trends with variations in deicer concentrations. As the deicer concentration increased, the energy ratio parameters were first reduced at the lowest concentration of 1:15 and subsequently increased. This finding was attributed to the higher mobility of the deicer solutions at low concentrations.

ER_1 and ER_2 found for aggregate-binder systems in the presence of $CaCl_2$ solutions of different concentrations exhibited a similar trend, as seen in the work of debonding values. It was concluded that $CaCl_2$ and moisture significantly reduced the energy parameters, implying a decrease in the aggregate-binder systems' resistance to moisture-induced damage. Particularly notable reductions were observed for the 1:15 and 1:10 $CaCl_2$ concentrations.

Using salt solutions at their lowest concentration (1:15) also resulted in lower energy ratio parameters than higher concentrations, indicating it may lead to more severe moisture-induced damage than when the deicer is diluted. However, as the deicers' concentration increased, the energy ratio parameters increased, with the highest ER_1 and ER_2 observed for the 1:0 salt concentration.

Table 4.11 Energy ratio values for PG 58-34 asphalt binder, quartzite aggregate, and salt solutions

Aqueous Salt Concentration (Eutectic Solution: Water)	ER_1			ER_2		
	$CaCl_2$	$MgCl_2$	NaCl	$CaCl_2$	$MgCl_2$	NaCl
0:1 (pure water without salt)	0.85			0.37		
1:15	0.58	0.50	0.58	0.25	0.22	0.25
1:10	0.62	0.73	0.62	0.27	0.32	0.27
1:4	0.70	0.89	0.65	0.30	0.39	0.28
1:0	0.71	4.45	0.85	0.31	1.93	0.37

4.3 Tensile Strength Ratio (TSR) Test

The indirect-measured tensile strength (ITS) values of dry specimens and those conditioned with different types of salt solutions of different concentrations, namely 0:1 (pure water), 1:10, and 1:4, subjected to seven F-T cycles were measured to determine the moisture-induced damage potential of the asphalt mix specimens. The average tensile strength values measured for dry and moisture-conditioned specimens and their TSR values are summarized in Table 4.12.

It was observed that the tensile strength values measured for dry specimens and those conditioned with pure water and $CaCl_2$ solutions of 1:10 and 1:4 concentrations subjected to F-T cycles were 884.6, 723.0, 665.8, and 686.9 kPa, respectively. Additionally, the TSR values for specimens conditioned with water, 1:10, 1:4 solutions, and seven F-T cycles were found to be 0.82, 0.75, and 0.78, respectively. This finding indicated the tensile strength values for conditioned specimens with water subjected to seven F-T cycles exhibited an 18.3% reduction compared to the dry specimens. This tensile strength loss was 24.7 and 22.3% for specimens conditioned with $CaCl_2$ solutions with 1:10 and 1:4 concentrations subjected to seven F-T cycles, respectively. Hence, it can be suggested that the presence of $CaCl_2$ had a damaging effect on the tensile strength of the mix specimens, while the worst cases were observed for the 1:10 and 1:4 concentrations, respectively, for which the TSR values dropped below the minimum requirement of 0.8 (Wen et al., 2013; Farooq et al., 2018; AASHTO, 2022a). A TSR value of less than the minimum requirement 0.8 indicates susceptibility to moisture-induced damage. This test's findings agreed with the results of the SFE method, indicating that while the presence of $CaCl_2$ increased the moisture-induced damage potential of the mix, the 1:10 concentration had the most damaging effect. Due to the difference in osmotic pressure, Ca^{2+} and Cl^- ions in $CaCl_2$ solutions can permeate the asphalt mix specimen's internal structure. In general, in lower concentrations, due to higher degrees of water saturation and osmotic pressure, the migration of water and $CaCl_2$ ions into the internal structure of the mix is facilitated (Wu et al., 2023). At concentrations higher than 1:10, a higher amount of salt may precipitate within the pores and channels of the HMA specimens, increasing the asphalt mix's density. Therefore, water and salt ion infiltration may be mitigated (Wu et al., 2023). In addition, the presence of $CaCl_2$ decreases the solution's freezing point. As a result, ice formed at higher concentrations would be weaker than those formed in lower concentrations, resulting in relatively lower stress subjected to the HMA specimen (Wu et al., 2023; Yang et al., 2020; Coussy and Monteiro, 2008).

The average tensile strength values for mix specimens conditioned with NaCl solutions at concentrations 1:10 and 1:4 and F-T cycles were identical to those conditioned with pure water (0:1) and F-T cycles, exhibiting an 18% decrease compared to the dry specimens. This finding indicates that NaCl had little to no effect on the specimens' average tensile strength values.

Mix specimens conditioned with $MgCl_2$ solutions at concentrations of 0:1, 1:10, and 1:4 had average tensile strength values of 18, 14, and 11% less than the dry specimens, respectively. This suggests higher $MgCl_2$ concentrations resulted in average tensile strength values that were comparatively higher than dry specimens.

These findings indicate that moisture-conditioned specimens conditioned with different deicer solutions and F-T cycles had the highest TSR value for $MgCl_2$ aqueous solution with 1:4 concentration (0.89), followed by $MgCl_2$ aqueous solution with 1:10 concentration (0.86), and equal values for NaCl aqueous solution with 1:10, and 1:4 concentrations, and pure water (0.82). However, CaCl2 deicer was found to have the most detrimental effect on TSR values compared to other salts. The phase diagram of the deicers at different temperatures and solution concentrations demonstrates that, at the same concentration, $MgCl_2$ has a higher ability to lower freezing point temperatures than NaCl and $CaCl_2$ (Ketcham et al., 1996). Therefore, the higher effectiveness of $MgCl_2$ in lowering the freezing point has likely contributed to less ice formation during F-T cycles, resulting in an improvement of average tensile strength.

While specimens conditioned with $MgCl_2$ and NaCl deicers may have contained a mix of ice and solution within the mix system during the F-T process, ice formation may have been more pronounced in the case of NaCl, resulting in an increase in expansion stress and, consequently, a decrease in tensile strength (Wu et al., 2023). At the 1:4 $MgCl_2$ concentration, however, the formed ice may have been weaker and exerted less tension on the mix (Goh et al., 2011; Wu et al., 2023). Moreover, at higher concentrations, more $MgCl_2$ may have precipitated in the pores and channels of the specimens, increasing the specimen's density, partially obstructing water and ion infiltration, and reducing the moisture-induced damage potential. The similarity of the trends observed for the TSR results and the energy ratio parameters confirms both methods validate the same conclusions.

Table 4.12 Summary of ITS and TSR values specimens prepared using HMA conditioned using different concentrations of deicer salts and F-T cycles

Salt Type	Conditioning Solution Volumetric Eutectic Salt Solution:Water	F-T Cycles	ITS (kPa)	COV (%)	TSR (ITS_{Wet}/ITS_{Dry})
None	No Conditioning (dry)	0	884.6	1.4%	-
	0:1 (pure water)	7	723.0	6.3%	0.82
$CaCl_2$	1:10	7	665.8	0.9%	0.75
	1:4	7	686.9	2.8%	0.78
$MgCl_2$	1:10	7	756.7	1.6%	0.86
	1:4	7	783.9	4.7%	0.89
NaCl	1:10	7	726.6	2.0%	0.82
	1:4	7	722.6	0.5%	0.82

4.4 Hamburg Wheel Tracker (HWT) Test

Rut depth values with the numbers of wheel passes, inverse creep slope, and SIP values measured for dry specimens and those conditioned with aqueous salt solutions of different concentrations (eutectic solution: water), namely 0:1, 1:10, and 1:4, subjected to seven F-T cycles are presented in Table 4.13. Table 4.13 shows the maximum corrected post-SIP rut depth measured for dry mix specimens and those conditioned with pure water and seven F-T cycles were 10.5 and 10.9 mm, respectively.

The maximum corrected post-SIP rut depth measured for mix specimens moisture-conditioned with $CaCl_2$ solutions of 1:10 and 1:4 concentrations subjected to seven F-T cycles are 10.9, 14.8, and 10.7 mm, respectively. This indicates the rutting resistance of the PG 58-34 HMA specimens conditioned with $CaCl_2$ solution of 0:1 (pure water), 1:10, and 1:4 concentrations deteriorated by 3.8, 41.0, and 1.9%, respectively, compared to the dry specimens. Therefore, $CaCl_2$ exacerbates the rutting, and it is evident that the worst case is when a salt concentration of 1:10 is used. Additionally, at the 1:10 concentration, the corrected rut depth value (14.8 mm) exceeds the rutting failure criteria of 12.5 mm, the maximum allowable rut depth. The moisture and aggressive chloride ions penetrating the HMA specimen's internal structure and infiltrating the aggregate-binder interface may weaken adhesion at this interface and reduce the moisture-induced damage and rutting resistance. Additionally, $CaCl_2$ crystallization may result in expansion stress and can exacerbate the damage (Feng et al., 2010). However, high salt concentrations (1:4 in this case) may have improved rutting resistance (Jiang et al., 2022). This observation confirms trends observed in other tests, such as TSR, and the results from energy ratio parameters. For all four conditions, specimens underwent stripping, which occurred at 14,847, 13,044, 10,025, and 12,558 passes for dry HMA specimens, and HMA specimens conditioned with $CaCl_2$ solutions with concentrations of 0:1 (pure water), 1:10, and 1:4 subjected to seven F-T cycles respectively. This finding indicates the stripping occurred at fewer passes in specimens subjected to the 1:10 concentration than the other specimens, followed by specimens conditioned with 1:4 concentration, water, and dry specimens, respectively. The inverse creep slope values of the mix specimens conditioned with $CaCl_2$ solutions with concentrations of 0:1 (pure water), 1:10, and 1:4 subjected to seven F-T cycles were 2500, 3333, 1666, and 2500 passes/mm, respectively. Therefore, in the presence of the 1:10 concentration of $CaCl_2$ solution, fewer passes resulted in 1 mm of traffic-induced rutting compared to the 1:4 concentration, and hence, $CaCl_2$ solution with 1:10 concentration decreased the resistance of the asphalt mix to traffic-induced creep, the second stage of rutting.

It was observed that the maximum rut depths measured for the specimens conditioned with $MgCl_2$ and NaCl solutions of 1:10 and 1:4 concentrations and seven F-T cycles were 10.0, 14.8, 11.3, and 11.6 mm, respectively. Thus, the rutting resistance of the conditioned mix specimens increased by 1.9% and 5.7% for water and $MgCl_2$ 1:10 solutions, respectively, whereas it decreased by 39.6, 6.6, and 9.4% for specimens conditioned with $MgCl_2$ solution at 1:4 concentration, NaCl solution at 1:10 and 1:4 concentrations, respectively. Therefore, the $MgCl_2$ salt with a 1:4 solution concentration had the most detrimental impact on rutting resistance (39.6%), followed by the NaCl 1:4 (9.4%) and NaCl 1:10 (6.6%) solutions. Consequently, the higher concentration of $MgCl_2$ led to a higher susceptibility to rutting compared to dry specimens. In high-temperature conditions, NaCl crystals may function as lubricants between aggregate and binder and reduce their resistance to rutting (Zhang et al., 2019).

The difference in results between the HWT test, the BBS test, and the findings of the SFE technique can be attributed to factors specific to this test. The aggregate-binder interfaces in asphalt mixes are subjected to tensile and shear stress during the HWT test, and the BBS test does not characterize this aspect. Therefore, the HWT test may contribute to failure mechanisms different from the BBS test. Additionally, the porous nature of the specimens and the high temperature at which the test is conducted are not present in the other methods and may result in a significant impact on the mechanisms involved in moisture-induced damage.

The inverse creep slope values were found to be 2,500, 3,333, 3,333, 1,429, 2,500, and 2,000 passes/mm for dry mix specimens and those conditioned with deicer aqueous solutions at different concentrations, namely 0:1 (pure water), $MgCl_2$ 1:10 and 1:4, and NaCl 1:10 and 1:4, subjected to seven F-T cycles, respectively. The specimens conditioned with water and $MgCl_2$ solution at 1:10 concentration and subjected to F-T cycles exhibited the highest inverse creep slope values, indicating they were more resistant to traffic-induced creep. The inverse creep slope values for the mix specimens conditioned with NaCl solutions were very close or identical to those of the dry specimens, indicating overall conditioning

with NaCl solution did not significantly affect their secondary rutting stage. However, the highest concentration of $MgCl_2$ (1:4) caused the most traffic-induced creep in mix specimens conditioned with this solution. The stripping inflection points (SIP) were detected for all the tested specimens, indicating this mix is susceptible to rutting overall. The SIP for dry mix specimens and those conditioned with deicer aqueous solutions of different concentrations, namely pure water (0:1), $MgCl_2$ 1:10 and 1:4, and NaCl 1:10 and 1:4, subjected to F-T cycles were 12,389, 12,652, 14,413, 9,381, 12,082, and 7,000 passes (Figure 6.14). Therefore, it is suggested that the stripping mechanism was initiated earlier at higher $MgCl_2$ and NaCl concentrations than lower concentrations, with NaCl 1:4 having the most detrimental effect on stripping initiation.

Table 4.13 Summary of rut depths, inverse creep slopes, and SIP measured for different dry and moisture-conditioned asphalt mixes

Salt Type	Conditioning Solution Volumetric Eutectic Salt Solution:Water	F-T Cycles	Measured Permanent Deformation (mm)				Inverse Creep Slope (pass/mm)	SIP (passes)
			Number of Wheel Passes					
			5,000	10,000	15,000	20,000		
None	Dry (no moisture)	0	4.5	6.4	8.5*	10.5*	2,500	14,847
	0:1 (pure water)	7	6.2	7.6	9.6*	10.9*	3,333	13,044
$CaCl_2$	1:10	7	5.7	9.3	11.8*	14.8*	1,666	10,025
	1:4	7	4.6	6.9	8.2*	10.7*	2,500	12,558
$MgCl_2$	1:10	7	4.6	6.4	8.3*	10.0*	3,333	14,413
	1:4	7	5.1	8.1*	11.5*	14.6*	1,429	9,381
NaCl	1:10	7	4.5	6.8	9.3*	11.3*	2,500	12,082
	1:4	7	5.1	8.4*	9.3*	11.6*	2,000	7,000

*Corrected post-SIP rut depth

4.5 Semicircular Bend (SCB) Test

Table 4.14 presents the J_c values measured for dry SCB specimens and those conditioned with aqueous salt solutions of different concentrations (eutectic solution: water), namely 0:1, 1:10, and 1:4 subjected to seven F-T cycles.

From Table 4.14, it is evident that the J_c value was reduced by 14.9, 26.9 and 22.8% for HMA specimens conditioned with solutions of 0:1 (pure water), 1:10, and 1:4 concentrations of $CaCl_2$, respectively, compared to the dry specimens. The lowest J_c value was observed for the $CaCl_2$ having a concentration of 1:10 (0.70 kJ/m^2); however, it was still higher than the values (0.50 kJ/m^2) recommended by ASTM D 8044 required for adequate crack resistance in mixes (ASTM, 2017). Given that a higher J_c value means a higher resistance to the formation and propagation of cracks in an asphalt mix, it is reasonable to expect that dry specimens followed by specimens moisture-conditioned with water and aqueous $CaCl_2$ solutions of 1:4 and 1:10 concentrations would have stronger resistance to cracking respectively.

The previously mentioned mechanisms can explain the findings of the SCB test. The migration of $CaCl_2$ ions into the HMA's internal structure can promote the emulsification of the asphalt binder and the dissolution of polar chemical groups within the asphalt binder, leading to the chemical aging of the asphalt mix. Additionally, during the dissolution and aging process, the decreased light components and increased heavy components of asphalt binder can increase stiffness (Cheng et al., 2023). Combined with the increased stiffness of the asphalt binder induced by F-T cycles, there is an increased risk of thermal stress buildup and micro-crack progression (Pang et al., 2018; Ma et al., 2011; Lei et al., 2015; Kavussi et

al., 2020). As a result, at the low concentration of 1:10, the potential for the formation and propagation of cracks was the highest.

This finding also suggests specimens conditioned with $CaCl_2$ concentrations of 0:1 (pure water), 1:4, and 1:10, respectively, were less susceptible to moisture-induced damage that could contribute to cracking. The energy ratio parameters supported this observation, with water exhibiting the highest energy ratio parameters, followed by the 1:4 and 1:10 solutions, respectively. A higher energy ratio parameter indicates increased resistance to moisture-induced damage (Bhasin et al., 2006). Additionally, the trend observed in the SCB test confirmed results of the TSR and HWT tests.

From Table 4.14, it was also observed that the J_c values measured for mix specimens conditioned with aqueous solutions of different concentrations, namely pure water (0:1), $MgCl_2$ solution at 1:10 and 1:4 concentrations subjected to seven F-T cycles, were 0.82, 0.86 and 0.83 respectively. The J_c values for mix specimens conditioned with NaCl solutions at 1:10 and 1:4 concentrations and seven F-T cycles were found to be 0.74 and 0.78, respectively. More notably, the reductions in J_c values for specimens conditioned with water, $MgCl_2$, and NaCl solution at 1:10 and 1:4 concentrations were, respectively, 15.0, 10.0, 13.1, 22.7, and 18.5% lower than that of dry specimens. Therefore, overall, conditioning the asphalt mix specimens with deicer solutions of different concentrations resulted in a reduction in J_c values, hence indicating higher susceptibility to the formation and propagation of cracks. This reduction was most significant for NaCl solutions at 1:10 (22.7%) and 1:4 (18.5%) concentrations. This observation can be explained by the erosion effect of chloride ions, which promotes the dissolution of polar chemical groups in binders. Consequently, the binder undergoes aging during the moisture-conditioning process and F-T cycles, increasing its brittleness and susceptibility to fracture (Zhang et al., 2022b; Guo et al., 2019; Long et al., 2022). The energy ratio parameters suggest a higher moisture-induced damage potential due to NaCl solutions than $MgCl_2$ solutions, which may have influenced the adhesive and cohesive bonds, resulting in lower fracture energy and higher propagation of cracks in specimens conditioned with NaCl than $MgCl_2$. It is important to note that despite the reduction in the J_c value for conditioned value, the values were higher than the minimum acceptable value of J_c (0.5 kJ/m^2) as determined by ASTM D8044 standard procedure (ASTM, 2017).

Table 4.14 Summary of rut depths, inverse creep slopes, and SIP measured for different dry and moisture-conditioned asphalt mixes

Salt Type	Conditioning Solution Volumetric Eutectic Salt Solution:Water	F-T Cycles	Critical Strain Energy Release Rate, Jc (kJ/m^2)
None	Dry (no moisture)	0	0.96
	0:1 (pure water)	7	0.82
$CaCl_2$	1:10	7	0.70
	1:4	7	0.74
$MgCl_2$	1:10	7	0.86
	1:4	7	0.83
NaCl	1:10	7	0.74
	1:4	7	0.78

5. CONCLUSIONS AND RECOMMENDATIONS

In this study, a multiscale characterization approach was used to investigate the effect of different deicing salts, namely $CaCl_2$, $MgCl_2$, and NaCl, used with various concentrations and freeze-thaw (F-T) cycles on the adhesion and debonding of aggregate-binder systems. The following conclusions are based on the findings, observations, and analysis from the tests conducted in this study.

1. In general, conditioning the aggregate-binder specimens with moisture and salt solutions reduced the pull-off strength values due to the weakening of cohesive bonds within the asphalt binder.

2. The crystallization of $CaCl_2$, resulting in the expansion of internal voids within the asphalt binder and the formation of micro-cracks in the asphalt binder, providing pathways for moisture infiltration, compromised the cohesive tensile strength.

3. The high concentration of $MgCl_2$ had a negative effect on the adhesive bonds, while NaCl negatively affected cohesive bonds. The weakening of the aggregate-binder interface adhesive bond was attributed to moisture infiltration into the asphalt binder via adsorption, replacement, and diffusion mechanisms. The mechanisms responsible for cohesive failure were salt crystallization due to F-T cycles, asphalt binder chemical aging, and increased brittleness.

4. Overall, specimens conditioned with NaCl solutions exhibited higher POS and PSR values than those subjected to $MgCl_2$ solutions. This finding was attributed to the Mg^{2+} lower atomic radius than the Na^+ ion, which may result in its more effective penetration into the interface.

5. The chemical aging and dissolution of the asphalt binder's polar chemical groups were linked to the asphalt binder's increased stiffness and reduced cohesive bond.

6. The presence of $CaCl_2$ solutions reduced the work of debonding and energy ratio parameters, with the lowest values observed at the concentration of 1:15. This was attributed to the increased mobility of the solution, which facilitates the transportation and displacement of the water-soluble layer and lighter bitumen binder components.

7. The total SFE of $MgCl_2$ solutions increased as the concentration increased, in contrast to NaCl, where an increase in concentration led to a decrease in the total SFE component.

8. The lowest $MgCl_2$ and NaCl concentrations (1:15) exhibited the lowest energy ratio parameters for both deicers and, therefore, the highest moisture-induced damage potential. High mobility of low-concentration solutions may facilitate the migration and displacement of light fractions and water-soluble layers of the asphalt binder.

9. NaCl solutions had a more detrimental effect on the cracking resistance of the mixes than $MgCl_2$.

10. The highest rutting was observed for the highest concentrations of salts. Additionally, the highest concentration of $MgCl_2$ caused the most traffic-induced creep in mix specimens conditioned with this solution, while the specimens conditioned with the highest concentration of NaCl had an increased stripping potential.

11. The higher effectiveness of $MgCl_2$ in lowering the freezing point has likely contributed to less ice formation during F-T cycles, improving average tensile strength and TSR values.

12. Energy ratio parameters and results from SCB, HWT, and TSR tests were found to agree, indicating the aqueous salt solutions with low concentrations of 1:15 and 1:10 had the most damaging effect.

The adhesion, debonding, and moisture-induced damage mechanisms and their evolution under the influence of three chloride-based deicers and environmental conditions in cold climates were studied by applying a comprehensive and multiscale material characterization and testing program. The following recommendations are suggested for future studies based on the study's limitations and observations.

1. Constructing a test section in cold regions (e.g., South Dakota) where periodical pavement monitoring and distress mapping are recommended to be carried out to compare laboratory findings with those observed in the field is recommended. Additionally, cores are recommended to be periodically extracted from the field test section and tested in the lab. These field observations can help calibrate laboratory findings to predict the durability of the asphalt mixes in cold regions more accurately by utilizing the laboratory test results.

2. Alternative methods for determining the aggregates' SFE components, such as a universal sorption device and dynamic vapor sorption, are recommended as they can predict the SFE components of aggregates with high accuracy.

3. It is recommended that the effects of deicers and F-T cycles on asphalt binder's rheology be studied at low, intermediate, and high temperatures.

4. It is recommended that the effect of deicers and F-T cycles on the resistance of asphalt mixes to low-temperature cracking be determined using a fracture energy-based characterization technique such as the disk-shaped compact tension (DCT) test.

5. Conducting a chemical analysis on asphalt binders is recommended to determine the effect of subjecting them to different deicer solutions and F-T cycles on their chemical aging rate.

6. REFERENCES

[1] AASHTO M 323 (2017a). Standard Specification for Superpave Volumetric Mix Design. Standard Specifications for Transportation Materials and Methods of Sampling and Testing, American Association of State Highway and Transportation Officials (AASHTO), Washington, D.C.

[2] AASHTO R 35 (2017b). Standard Practice for Superpave Volumetric Design for Asphalt Mixtures. Standard Specifications for Transportation Materials and Methods of Sampling and Testing, American Association of State Highway and Transportation Officials (AASHTO), Washington, D.C.

[3] AASHTO R 30 (2016). Standard Practice for Mixture Conditioning of Hot Mix Asphalt (HMA). Standard Specifications for Transportation Materials and Methods of Sampling and Testing, American Association of State Highway and Transportation Officials (AASHTO), Washington, D.C.

[4] AASHTO T 283 (2022a). Standard Method of Test for Resistance of Compacted Asphalt Mixtures to Moisture-Induced Damage. Standard Specifications for Transportation Materials and Methods of Sampling and Testing, American Association of State Highway and Transportation Officials (AASHTO), Washington, D.C.

[5] AASHTO T 324 (2022b). Standard Method of Test for Hamburg Wheel-Track Testing of Compacted Hot Mix Asphalt (HMA). Standard Specifications for Transportation Materials and Methods of Sampling and Testing, American Association of State Highway and Transportation Officials (AASHTO), Washington, D.C.

[6] AASHTO T 361 (2022c). Standard Method of Test for Determining Asphalt Binder Bond Strength by Means of the Binder Bond Strength (BBS) Test. Standard Specifications for Transportation Materials and Methods of Sampling and Testing, American Association of State Highway and Transportation Officials (AASHTO), Washington, D.C.

[7] ASTM D8044 (2017). Standard Test Method for Evaluation of Asphalt Mixture Cracking Resistance using the Semi-Circular Bend Test (SCB) at Intermediate Temperatures. 2016 Annual Book of ASTM Standards, ASTM International, West Conshohocken, PA.

[8] Mihandoust, M. and Ghabchi, R. (2024). Multiscale evaluation of asphalt binder-aggregate interface exposed to sodium chloride deicer. *International Journal of Pavement Engineering*, *25*(1), p.2370555.

[9] Mihandoust, M. and Ghabchi, R. (2023). Mechanical, thermodynamical, and microstructural characterization of adhesion evolution in asphalt binder-aggregate interface subjected to calcium chloride deicer. *Construction and Building Materials*, *408*, p.133663.

[10] Ghabchi, R., Singh, D., Zaman, M. and Hossain, Z. (2016). Micro-structural analysis of moisture-induced damage potential of asphalt mixes containing RAP. *Journal of Testing and Evaluation*, *44*(1), pp.194-205.

[11] Ghabchi, R. and Castro, M.P. (2022). Characterisation of a hybrid plant-based asphalt binder replacement with high reactive phenolic monomer content. *International Journal of Pavement Engineering*, *23*(13), pp.4675-4696.

[12] Ghabchi, R. and Castro, M.P.P. (2021a). Evaluation of a biofuel residue-derived recycling agent with a low carbon footprint. *Transportation Engineering*, *5*, p.100085.

[13] Ghabchi, R. and Castro, M.P.P., 2021b. Effect of laboratory-produced cellulose nanofiber as an additive on performance of asphalt binders and mixes. *Construction and Building Materials*, *286*, p.122922.

[14] Ghabchi, R., Singh, D. and Zaman, M. (2014). Evaluation of moisture susceptibility of asphalt mixes containing RAP and different types of aggregates and asphalt binders using the surface free energy method. *Construction and Building Materials*, *73*, pp.479-489.

[15] MnDOT (Minnesota Department of Transportation) (2019). Maintaining Minnesota's Highways, Online: https://www.dot.state.mn.us/maintenance/faq.html (Accessed: May 2019).

[16] NHDES (New Hampshire Department of Environmental Services) (2019). Road Salt and Water Quality Fact Sheet, Online: http://des.nh.gov/organization/commissioner/pip/factsheets/wmb/documents/wmb-4.pdf (Accessed: May 2019).
[17] USGS (U.S. Geological Survey) (2016a). "Mineral Commodity Summaries 2016, Stone (Crushed)," Online: https://minerals.usgs.gov/minerals/pubs/commodity/stone_ crushed/mcs-2016-stonc.pdf (Accessed: May 2019).
[18] USGS (U.S. Geological Survey) (2015). Minerals Yearbook Magnesium Compounds. Online: https://minerals.usgs.gov/minerals/pubs/commodity/ magnesium/myb1-2015-mgcom.pdf (Accessed: May 2019).
[19] USGS (U.S. Geological Survey) (2016b). Mineral Commodity Summaries, Potash. Online: https://minerals.usgs.gov/minerals/pubs/commodity/potash/mcs-2016- potas.pdf (Accessed: May 2019).
[20] Sumsion, E. S., and Guthrie, W. S. (2013). Physical and chemical effects of deicers on concrete pavement: Literature review. Report No. UT-13.09, Utah Department of Transportation, 4501 South 2700 West, P.O. Box 148410, Salt Lake City, UT 84114-8410.
[21] AGS (American Geoscience Society) (2017). Roadway deicing in the United States – Fact Sheet. Online: https://www.americangeosciences.org/sites/default/files/CI_Factsheet_2017_3_Deicing_170712.pdf (Accessed: May 2019).
[22] Hassan Y, Halim AOAE, Razaqpur AG, Bekheet W, and Farha M. (2002). Effects of runway deicer on pavement materials and mixes: comparison with road salt. *Journal of Transport Engineering*, 128(4):385–91
[23] Goh, S. W., Akin, M., You, Z., and Shi, X. (2011). Effect of deicing solutions on the tensile strength of micro-or nano-modified asphalt mixture. *Construction and Building Materials*, *25*(1), 195-200.
[24] Shi X, Akin M, Pan T, Fay L, Liu Y, Yang Z. (2009). Deicer impacts on pavement materials: introduction and recent developments. Open Civil Engineering Journal, 3:16–27.
[25] Ali, S.A., Zaman, M., Ghabchi, R., Rahman, M.A., Ghos, S. and Rani, S. (2022). Effect of additives and aging on moisture-induced damage potential of asphalt mixes using surface free energy and laboratory-based performance tests. International Journal of Pavement Engineering, 23(2), pp.285-296.
[26] Alvarez, A. E., Ovalles, E., and Martin, A. E. (2012). Comparison of asphalt rubber-aggregate and polymer modified asphalt–aggregate systems in terms of surface free energy and energy indices. Construction and Building Materials, 35, 385-392.
[27] Arabani, M., and Hamedi, G. H. (2011). Using the surface free energy method to evaluate the effects of polymeric aggregate treatment on moisture damage in hot-mix asphalt. Journal of Materials in Civil Engineering, 23(6), 802-811.
[28] Asif, S. A., Ahmed, N., Hayat, A., Hussan, S., Shabbir, F., and Mehmood, K. (2018). Study of adhesion characteristics of different bitumen–aggregate combinations using bitumen bond strength test. Journal of the Chinese Institute of Engineers, 41(5), 430-440.
[29] Atkins, P., and De Paula, J. (2006). Physical chemistry (Vol. 1). Macmillan.
[30] Behbahani, H., Hamedi, G. H., and Gilani, V. N. M. (2020). Predictive model of modified asphalt mixtures with nano hydrated lime to increase resistance to moisture and fatigue damages by the use of deicing agents. Construction and Building Materials, 265, 120353.
[31] Bhasin, A., and Little, D. N. (2007). Characterization of aggregate surface energy using the universal sorption device. Journal of Materials in Civil Engineering, 19(8), 634-641.
[32] Bhasin, A., and Little, D. N. (2009). Application of microcalorimeter to characterize adhesion between asphalt binders and aggregates. Journal of Materials in Civil Engineering, 21(6), 235-243.
[33] Bhasin, A., Howson, J., Masad, E., Little, D. N., and Lytton, R. L. (2007a). Effect of modification processes on bond energy of asphalt binders. Transportation Research Record, 1998(1), 29-37.

[34] Bhasin, A., Little, D. N., Vasconcelos, K. L., and Masad, E. (2007b). Surface Free Energy to Identify Moisture Sensitivity of Materials for Asphalt Mixes. Transportation Research Record, 2001(1), 37-45. https://doi.org/10.3141/2001-05
[35] Canestrari, F., Cardone, F., Graziani, A., Santagata, F. A., and Bahia, H. U. (2010). Adhesive and cohesive properties of asphalt-aggregate systems subjected to moisture damage. Road Materials and Pavement Design, 11(sup1), 11-32.
[36] Caro, S., Masad, E., Bhasin, A., and Little, D. (2010a). Coupled micromechanical model of moisture-induced damage in asphalt mixtures. Journal of Materials in Civil Engineering, 22(4), 380-388.
[37] Caro, S., Masad, E., Bhasin, A., and Little, D. (2010b). Micromechanical modeling of the influence of material properties on moisture-induced damage in asphalt mixtures. Construction and Building Materials, 24(7), 1184-1192.
[38] Chen, X., Ren, D., Tian, G., Xu, J., Ali, R., and Ai, C. (2023). Investigation on moisture damage resistance of asphalt pavement in salt and acid erosion environments based on Multiscale analysis. Construction and Building Materials, 366, 130177.
[39] Choi, Y. (2007). Case study and test method review on moisture damage (No. AP-T76/07).
[40] Cui, S., Blackman, B. R., Kinloch, A. J., and Taylor, A. C. (2014). Durability of asphalt mixtures: Effect of aggregate type and adhesion promoters. International Journal of Adhesion and Adhesives, 54, 100-111.
[41] Cui, Y., Chen, D., Feng, L., and Wang, L. (2017). Effects of salt freeze damage on the viscoelastic performance of asphalt mortar. Ceramics-Silikáty, 61(3), 257-266.
[42] Drelich, J. (1997). The Effect of Drop (Bubble) Size on Contact Angle at Solid Surfaces. The Journal of Adhesion, 63(1-3), 31-51. https://doi.org/10.1080/00218469708015212
[43] Du, Z., and Zhu, X. (2019). Molecular dynamics simulation to investigate the adhesion and diffusion of asphalt binder on aggregate surfaces. Transportation Research Record, 2673(4), 500-512.
[44] Fakhri, M., Javadi, S., Sedghi, R., Arzjani, D., & Zarrinpour, Y. (2019). Effects of deicing agents on moisture susceptibility of the WMA containing recycled crumb rubber. Construction and Building Materials, 227, 116581.
[45] Feng, D., Yi, J., Wang, D., and Chen, L. (2010). Impact of salt and freeze–thaw cycles on performance of asphalt mixtures in coastal frozen region of China. Cold Regions Science and Technology, 62(1), 34-41.
[46] FHWA (Federal Highway Administration). (2023). Road weather management program—snow and ice. Last modified Feb 1st. Washington, DC https://ops.fhwa.dot.gov/weather/weather_events/snow_ice.htm
[47] Good, R. J. (1992). Contact angle, wetting, and adhesion: a critical review. Journal of adhesion science and technology, 6(12), 1269-1302.
[48] Good, R. J., and Srivatsa, N. R. Islam. M., Huang, HTL and van Oss, CJ, (1990). Theory of the Add-Base Hydrogen Bonding Interactions, Contact Angles, and the Hysteresis of Wetting: Application to Coal and Graphite Surfaces. Journal of Adhesion Science and Technology, 4(8), 607-617.
[49] Good, R. J., and Van Oss, C. J. (1990). Modern Aspects of Wettability. Plenum Press, New York.
[50] Guo, Q., Li, G., Gao, Y., Wang, K., Dong, Z., Liu, F., and Zhu, H. (2019). Experimental investigation on bonding property of asphalt-aggregate interface under the actions of salt immersion and freeze-thaw cycles. Construction and Building Materials, 206, 590-599. https://doi.org/https://doi.org/10.1016/j.conbuildmat.2019.02.094
[51] Guo, Z., Wang, L., Feng, L., and Guo, Y. (2022a). Research on fatigue performance of composite crumb rubber modified asphalt mixture under freeze thaw cycles. Construction and Building Materials, 323, 126603.
[52] Habal, A., and Singh, D. (2022). Establishing threshold value of surface free energy and binder bond strength parameters for basaltic asphalt mixes. Road Materials and Pavement Design, 23(8), 1877-1899.

[53] Hamedi, G. H., and Moghadas Nejad, F. (2015). Using energy parameters based on the surface free energy concept to evaluate the moisture susceptibility of hot mix asphalt. Road Materials and Pavement Design, 16(2), 239-255.
[54] Han, S., Yao, T., and Yang, X. (2019). Preparation and anti-icing properties of a hydrophobic emulsified asphalt coating. Construction and Building Materials, 220, 214-227.
[55] Hefer, A. W., Bhasin, A., and Little, D. N. (2006). Bitumen surface energy characterization using a contact angle approach. Journal of Materials in Civil Engineering, 18(6), 759-767.
[56] Howson, J. E. (2011). Relationship between surface free energy and total work of fracture of asphalt binder and asphalt binder-aggregate interfaces (Vol. 73, No. 03).
[57] Jiang-san, H., Lan, W., and Xin, L. (2022). Anti-fatigue performance of warm-mixed rubber powder modified asphalt mixture based on the DIC technique. Construction and Building Materials, 335, 127489.
[58] Juli-Gándara, L., Vega-Zamanillo, Á., and Calzada-Pérez, M. Á. (2019). Sodium chloride effect in the mechanical properties of the bituminous mixtures. Cold Regions Science and Technology, 164, 102776.
[59] Kakar, M. R., Hamzah, M. O., and Valentin, J. (2015). A review on moisture-induced damages of hot and warm mix asphalt and related investigations. Journal of Cleaner Production, 99, 39-58.
[60] Ketcham, S., Minsk, L. D., Blackburn, R. R., and Fleege, E. J. (1996). Manual of practice for an effective anti-icing program: a guide for highway winter maintenance personnel (No. FHWA-RD-95-202). United States. Federal Highway Administration.
[61] Kim, Y. R., Little, D. N., and Lytton, R. L. (2004). Effect of moisture damage on material properties and fatigue resistance of asphalt mixtures. Transportation Research Record, 1891(1), 48-54.
[62] Koc, M., and Bulut, R. (2014). Assessment of a sessile drop device and a new testing approach measuring contact angles on aggregates and asphalt binders. Journal of Materials in Civil Engineering, 26(3), 391-398.
[63] Kolesar, K. R., Mattson, C. N., Peterson, P. K., May, N. W., Prendergast, R. K., and Pratt, K. A. (2018). Increases in wintertime PM2. 5 sodium and chloride linked to snowfall and road salt application. Atmospheric Environment, 177, 195-202.
[64] Little, D. N., and Bhasin, A. (2007). Using surface energy measurements to select materials for asphalt pavement.
[65] Lottman, R. P. (1982). Laboratory test methods for predicting moisture-induced damage to asphalt concrete. Transportation research record, (843).
[66] Luo, S., and Yang, X. (2015). Performance evaluation of high-elastic asphalt mixture containing deicing agent Mafilon. Construction and Building Materials, 94, 494-501.
[67] Mishra, V., Singh, D., and Habal, A. (2020). Investigating the condition number approach to select probe liquids for evaluating surface free energy of bitumen. International Journal of Pavement Research and Technology, 13, 10-19.
[68] Moghadas Nejad, F., Hamedi, G. H., and Azarhoosh, A. R. (2013). Use of surface free energy method to evaluate effect of hydrate lime on moisture damage in hot-mix asphalt. Journal of Materials in Civil Engineering, 25(8), 1119-1126.
[69] Moraes, R., Velasquez, R., and Bahia, H. U. (2011). Measuring the effect of moisture on asphalt–aggregate bond with the bitumen bond strength test. Transportation Research Record, 2209(1), 70-81.
[70] Muthumani, A., Fay, L., and Shi, X. (2017). Agricultural by-products weaken the snow/ice bond to pavement and improve sunlight absorbance and longevity on road (No. 17-05584).
[71] NAPA (National Asphalt Pavement Association), 2023. Engineering Overview. https://www.asphaltpavement.org/expertise/engineering. Accessed on August 1, 2023.
[72] Nixon, W. A., and Williams, A. D. (2001). A guide for selecting anti-icing chemicals, version 1.0. IIHR Technical Rep, 420.
[73] Ogbon, W. A., Xu, H., Jiang, W., and Xing, C. (2022). Polymer-modified asphalt binders' properties deterioration under the action of chloride salt. Road Materials and Pavement Design, 1-21.

[74] Pang, L., Zhang, X., Wu, S., Ye, Y., and Li, Y. (2018). Influence of water solute exposure on the chemical evolution and rheological properties of asphalt. Materials, 11(6), 983.
[75] Prieve, D. C., Malone, S. M., Khair, A. S., Stout, R. F., and Kanj, M. Y. (2019). Diffusiophoresis of charged colloidal particles in the limit of very high salinity. Proceedings of the National Academy of Sciences, 116(37), 18257-18262.
[76] Qian, G., Yu, H., Jin, D., Bai, X., and Gong, X. (2021). Different water environment coupled with ultraviolet radiation on ageing of asphalt binder. Road Materials and Pavement Design, 22(10), 2410-2423.
[77] Safazadeh, F., Romero, P., Mohammad Asib, A. S., and VanFrank, K. (2022). Methods to evaluate intermediate temperature properties of asphalt mixtures by the semi-circular bending (SCB) test. Road Materials and Pavement Design, 23(7), 1694-1706.
[78] Sarsembayeva, A., and Collins, P. E. (2017). Evaluation of frost heave and moisture/chemical migration mechanisms in highway subsoil using a laboratory simulation method. Cold Regions Science and Technology, 133, 26-35.
[79] Shan, L., Li, Z., Tian, D., and Tan, Y. (2021). Effect of anti-icing additives on the stability of emulsified asphalt binders. Construction and Building Materials, 275, 121951.
[80] Soenen, H., Vansteenkiste, S., and Kara De Maeijer, P. (2020). Fundamental approaches to predict moisture damage in asphalt mixtures: State-of-the-art review. Infrastructures, 5(2), 20.
[81] Tarrer, A. R., Wagh, Vinay, (1991). The Effect of the Physical and Chemical Characteristics of the Aggregate on Bonding. No. SHRP-A/UIR-91e507. Strategic Highway Research Program, National Research Council, Washington, D.C.
[82] Tavassoti, P., & Baaj, H. (2020). Moisture Damage in Asphalt Concrete Mixtures: State of the Art and Critical Review of the Test Methods. In Transportation Association of Canada 2020 Conference and Exhibition-The Journey to Safer Roads.
[83] Teguedi, M. C., Toussaint, E., Blaysat, B., Moreira, S., Liandrat, S., and Grédiac, M. (2017). Towards the local expansion and contraction measurement of asphalt exposed to freeze-thaw cycles. Construction and Building Materials, 154, 438-450.
[84] Van Oss, C. J. (1994).Interfacial forces in aqueous media, Marcel Dekker, New York.
[85] Van Oss, C. J. (2002). Use of the combined Lifshitz–van der Waals and Lewis acid–base approaches in determining the apolar and polar contributions to surface and interfacial tensions and free energies. Journal of adhesion science and technology, 16(6), 669-677.
[86] Van Oss, C. J. (2008). The Properties of Water and Their Role in Colloidal and Biological Systems; Academic Press.
[87] Van Oss, C. J., Chaudhury, M. K., and Good, R. J. (1987). Monopolar surfaces. Advances in colloid and interface science, 28, 35-64.
[88] Van Oss, C. J., Chaudhury, M. K., and Good, R. J. (1988). Interfacial Lifshitz-van der Waals and polar interactions in macroscopic systems. Chemical reviews, 88(6), 927-941.
[89] Wåhlin, J., Leisinger, S., and Klein-Paste, A. (2014). The effect of sodium chloride solution on the hardness of compacted snow. Cold regions science and technology, 102, 1-7.
[90] Wang, F., Qin, X., Pang, W., & Wang, W. (2021). Performance deterioration of asphalt mixture under chloride salt erosion. Materials, 14(12), 3339.
[91] Wu, Z., Shi, C., Gao, P., Zhang, H., and Hu, X. (2023). Moisture Susceptibility of Asphalt Mixture Subjected to Chloride-Based Deicing Salt Solutions under Simulated Environmental Conditions. Journal of materials in civil engineering, 35(5), 04023052.
[92] Yan, C., Huang, W., and Lv, Q. (2016). Study on bond properties between RAP aggregates and virgin asphalt using Binder Bond Strength test and Fourier Transform Infrared spectroscopy. Construction and Building Materials, 124, 1-10.
[93] Yang, J., Zhu, X., Li, L., Ling, H., Zhou, P., Cheng, Z., and Du, Y. (2018). Prefabricated flexible conductive composite overlay for active deicing and snow melting. Journal of Materials in Civil Engineering, 30(11), 04018283.

[94] Yang, S. L., Baek, C., and Park, H. B. (2021). Effect of aging and moisture damage on fatigue cracking properties in asphalt mixtures. Applied Sciences, 11(22), 10543.
[95] Yee, T. S., and Hamzah, M. O. (2019). Evaluation of moisture susceptibility of asphalt-aggregate constituents subjected to direct tensile test using imaging technique. Construction and Building Materials, 227, 116642.
[96] Yin, F., Arambula, E., Lytton, R., Martin, A. E., and Cucalon, L. G. (2014). Novel method for moisture susceptibility and rutting evaluation using Hamburg wheel tracking test. Transportation Research Record, 2446(1), 1-7.
[97] Yin, F., Chen, C., West, R., Martin, A. E., and Arambula-Mercado, E. (2020). Determining the relationship among hamburg wheel-tracking test parameters and correlation to field performance of asphalt pavements. Transportation Research Record, 2674(4), 281-291.
[98] Young, T. (1805). III. An essay on the cohesion of fluids. Philosophical transactions of the royal society of London(95), 65-87.
[99] Zdziennicka, A., Szymczyk, K., Krawczyk, J., and Jańczuk, B. (2017). Some remarks on the solid surface tension determination from contact angle measurements. Applied Surface Science, 405, 88-101.
[100] Zettlemoyer, A. C. (1968). Hydrophobic surfaces. Journal of Colloid and Interface Science, 28(3-4), 343-369.
[101] Zhang, J., Airey, G. D., Grenfell, J., and Apeagyei, A. K. (2018). Moisture sensitivity examination of asphalt mixtures using thermodynamic, direct adhesion peel and compacted mixture mechanical tests. Road Materials and Pavement Design, 19(1), 120-138.
[102] Zhang, R., Tang, N., and Zhu, H. (2022a). The effect of sea salt solution erosion on cohesion, chemical and rheological properties of SBS modified asphalt. Construction and Building Materials, 318, 125923.
[103] Zhang, R., Tang, N., Deng, X., Zhu, H., Su, C., & Xi, Y. (2022b). Erosion mechanism of sea salt solution on the performance of SBS-modified asphalt mixtures. International Journal of Pavement Engineering, 1-9.
[104] Zhou, P., Wang, W., Zhu, L., Wang, H., and Ai, Y. (2021). Study on performance damage and mechanism analysis of asphalt under action of chloride salt erosion. Materials, 14(11), 3089.
[105] Wen, H., Bhusal, S., and Wen, B. (2013). Laboratory evaluation of waste cooking oil-based bioasphalt as an alternative binder for hot mix asphalt. Journal of Materials in Civil Engineering, 25(10), 1432-1437.
[106] Farooq, M. A., Mir, M. S., and Sharma, A. (2018). Laboratory study on use of RAP in WMA pavements using rejuvenator. Construction and Building Materials, 168, 61-72.
[107] Yang, H., Pang, L., Zou, Y., Liu, Q., & Xie, J. (2020). The effect of water solution erosion on rheological, cohesion and adhesion properties of asphalt. Construction and Building Materials, 246, 118465.
[108] Coussy, O., and Monteiro., P. J. (2008).“Poro elastic model for concrete exposed to freezing temperatures. Cem. Concr. Res.38 (1): 40–48.https://doi.org/10.1016/j.cemconres.2007.06.006.
[109] Goh, S. W., Akin, M., You, Z., and Shi, X. (2011). Effect of deicing solutions on the tensile strength of micro-or nano-modified asphalt mixture. Construction and Building Materials, 25(1), 195-200.
[110] Zhang, K., Li, W., & Han, F. (2019). Performance deterioration mechanism and improvement techniques of asphalt mixture in salty and humid environment. Construction and Building Materials, 208, 749-757.
[111] Cheng, Y., Wang, H., Wang, W., and Liang, J. (2023). Rheological evolution mechanisms of asphalt binder and mastic under freeze-thaw cycles. Construction and Building Materials, 372, 130780.
[112] Ma, T., Huang, X. M., Mahmoud, E., and Garibaldy, E. (2011). Effect of moisture on the aging behavior of asphalt binder. International Journal of Minerals, Metallurgy, and Materials, 18(4), 460-466.
[113] Lei, Z., Bahia, H., and Yi-qiu, T. (2015). Effect of bio-based and refined waste oil modifiers on low temperature performance of asphalt binders. Construction and building materials, 86, 95-100.

[114] Kavussi, A., Karimi, M. M., and Dehaghi, E. A. (2020). Effect of moisture and freeze-thaw damage on microwave healing of asphalt mixes. Construction and Building Materials, 254, 119268.
[115] Bhasin, A., Masad, E., Little, D., and Lytton, R. (2006). Limits on adhesive bond energy for improved resistance of hot-mix asphalt to moisture damage. Transportation Research Record, 1970(1), 2-13
[116] Long, Z., Guo, N., Tang, X., Ding, Y., You, L., and Xu, F. (2022). Microstructural evolution of asphalt induced by chloride salt erosion. Construction and Building Materials, 343, 128056.